

An-Najah National University

Faculty of Graduate studies

**ZnO nano-particle catalysts in contaminant degradation processes
with solar light**

Naked and supported systems

By

Hussam Ahmad Abdullah Amer

Supervisor

Prof. Hikmat Hilal

**This Thesis is Submitted in Partial Fulfillment of the Requirements
for the Degree of Master of Science in Chemistry, Faculty of Graduate
Studies, An-Najah National University, Nablus, Palestine.**

2012

**ZnO nano-particle catalysts in contaminant degradation processes
with solar light:**

Naked and supported systems

By

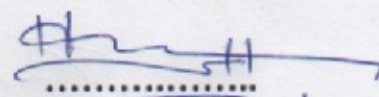
Hussam Ahmad Abdullah Amer

This Thesis was defended successfully on 6 /9 / 2012 and approved by:

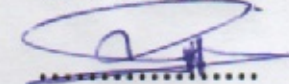
Defense Committee Members

signature

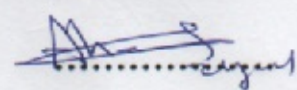
1. Dr. Prof. Hikmat Hilal (supervisor)



2. Dr. Wadie Sultan (External Examiner)



3. Dr. Ahed Zyoud (Internal Examiner)



DEDICATION

This thesis is especially dedicated to my mother, to my father, and to my wife (Samah).

ACKNOWLEDGEMENTS

I would like to thank and express my principal supervisor Prof. Hikmat Hilal. His brilliant academic guidance, continuous encouragement, patience, time, enthusiasm and support are greatly appreciated.

Thanks to King Abdullah Institute for nanotechnology and King Saud University for their collaboration in advanced sample analysis through Dr. Ismail Warad, also special thank to Dr. Warad for his efforts.

I would like to extend my appreciation and thanks to Prof. Dr. Guy Campet and to Dr. DaeHoon Park, both of ICMCB (University of Bordeaux), for assistance with X-ray Diffraction (XRD) and Scanning Electron Microscopy (SEM).

Thanks are due to French-Palestinian University Cooperation Program (Al-Magdisi) for financial support to this project and travel assistance to Bordeaux.

I would like to thank Dr. Iyad Saadeddin and Dr. Ahed Zyoud for continued help through out this work.

I am deeply grateful to my parents, sisters and brother for their support and encouragement all the time.

Finally, I would like to thank my mother, my father who passed away during the course of this work, and my wife.

الإقرار

أنا الموقع أدناه مقدم الرسالة التي تحت عنوان:

ZnO nano-particle catalysts in contaminant degradation processes with solar light:

Naked and supported systems

حفازات حبيبات أكسيد الزنك النانوية في تحطيم الملوثات بالضوء الشمسي: أهمية تثبيت الحفاز

أقر بأن ما اشتملت عليه الرسالة إنما هي من إنتاجي الشخصي باستثناء ما تمت الإشارة إليه
حيثما ورد، وان الرسالة ككل، أو أي جزء منها لم يقدم من قبل لنيل أية درجة علمية أو بحث
علمي أو بحثي لدى أية مؤسسة تعليمية أو بحثية أخرى.

Declaration

This work provided in this thesis, unless otherwise referenced, is the researcher's own work, and has not been submitted elsewhere for any other degree or qualification.

Students name :

اسم الطالب

Signature :

التوقيع :

Date:

التاريخ:

List of Contents

No.	Subject	Page
	Committee Decision	ii
	Dedication	v
	Acknowledgments	iv
	Declaration	vi
	List of Tables	ix
	List of Figures	x
	List of Abbreviations	xv
	Abstract	xvi
	CHAPTER 1:INTRODUCTION	1
1.1	Photo-Catalysis Overview	1
1.2	Photocatalyst Role in Contaminant Degradation	3
1.3	Why ZnO Rather Than TiO ₂	5
1.4	ZnO Nano-Particles	7
1.5	What's New on This Work?	8
	CHAPTER 2: EXPERIMENTAL	9
2.1	Materials and Reagents	9
2.2	Equipments	9
2.2.1	Measuring Devices	9
2.2.1.1	UV/ Vis Spectrophotometer	9
2.2.1.2	Fluorescence Spectrometry	10
2.2.1.3	Lux-meter	10
2.2.1.4	Scanning Electron Microscopy (SEM)	10
2.2.1.5	X-ray Diffraction (XRD)	10
2.2.2	Light Sources	11
2.2.2.1	Direct Sun Light	11
2.2.2.2	Concentrated Sun Light (by Mirrors)	11
2.2.2.3	UV Lamp	11
2.3	Solution Preparation	13
2.4	Materials Preparations Technique	14
2.4.1	ZnO Thin Films on Glass	14
2.4.2	ZnO Nano-Particles	15
2.4.2.1	Preparation by Sonication	16
2.4.2.2	Preparation Without Sonication	17
2.4.3	ZnO/AC	18
2.4.4	ZnO/Clay	19
2.4.5	ZnO/Sand	19

2.4.6	Annealing	19
2.5	Catalytic Experiment	20
	CHAPTER 3:RESULTS	24
3.1	Catalyst System Characterization	24
3.1.1	ZnO Nano-Particles Annealed and Non-Annealed	24
3.1.1.1	Absorption Spectra	24
3.1.1.2	Photoluminescence Emission	25
3.1.1.3	X-ray Diffraction (XRD)	28
3.1.2	Sand-Supported ZnO System	31
3.1.2.1	X-ray Diffraction (XRD)	31
3.1.3	Clay-Supported ZnO	32
3.1.3.1	X-ray Diffraction (XRD)	32
3.1.4	AC-Supported ZnO System Annealed and Non-Annealed	33
3.1.4.1	X-ray Diffraction (XRD)	33
3.1.4.2	Scanning Electron Microscopy (SEM)	34
3.2	Photodegradation Reaction	36
3.2.1	ZnO Nano-Particles Annealed and Non-Annealed	36
3.2.1.1	Effect of Temperature	39
3.2.1.2	Effect of Catalyst Concentration	41
3.2.1.3	Effect of Contaminant Concentration	42
3.2.1.4	Effect of Light Concentration	43
3.2.2	Sand-Supported ZnO System Annealed and Non-Annealed	44
3.2.2.1	Effect of pH	44
3.2.2.2	Effect of Temperature	46
3.2.2.3	Effect of Catalyst Concentration	47
3.2.2.4	Effect of Contaminant Concentration	49
3.2.2.5	Effect of Light Concentration	50
3.2.3	Clay-Supported ZnO System Annealed and Non-Annealed	51
3.2.3.1	Effect of Temperature	52

3.2.3.2	Effect of Catalyst Concentration	53
3.2.3.3	Effect of Contaminant Concentration	54
3.2.3.4	Effect of Light Concentration	55
3.2.4	AC-Supported ZnO System Annuals and Non-Annealed	56
3.2.4.1	Effect of Temperature	56
3.2.4.2	Effect of Catalyst Concentration	57
3.2.4.3	Effect of Contaminant Concentration	58
3.2.4.4	Effect of Light Concentration	58
3.2.5	Thin Film ZnO System	60
3.2.5.1	Effect of Light Concentration	60
	CHAPTER 4:DISCUSSIONS	60
4.1	General	62
4.2	Photoluminescence for ZnO Systems:	62
4.3	X-ray Diffraction (XRD) :	63
4.4	SEM Results:	64
4.5	Photocatalytic Degradation of MO	64
4.5.1	pH Effect.	65
4.5.2	Effect of Photoreaction Temperature.	65
4.5.3	Effect of Catalytic Concentration.	66
4.5.4	Effect of Contaminant Concentration.	67
4.5.5	Effect of Light Concentration.	67
4.6	Effect of Annealing	68
	CONCLUSIONS	70
	SUGGESTIONS FOR FURTHER WORK	71
	REFERENCES	72
	المخلص	ب

List of Tables

No.	Subject	Page
1	UV lamp specifications	12
2	Peak position and particle size values for different synthetic ZnO systems .	30
3	Values of T.N. and Q.Y. for MO degradation using different catalyst systems, after 40 min.	39
4	Photoluminescence emission spectra wavelength for ZnO systems.	62
5	Particle size values for different synthetic ZnO systems .	63

List of Figures

No.	Subject	Page
1.1	Mechanism of photo-catalysis.	3
2.1	Arrangement of photo-catalytic reactor.	12
2.2	Spectrograms for: a) halogen lamps b) sun light c) mercury vapor lamp	13
2.3	ZnO thin films on glass.	15
2.4	Sonication process for nano-crystalline ZnO preparation.	16
2.5	Preparation method for nanocrystalline ZnO	17
2.6	Precipitation method for nano-crystalline ZnO/AC preparation.	18
2.7	Adsorption of contaminant on a) ZnO/AC b) ZnO/Clay c) ZnO/Sand, in the dark.	21
2.8	ZnO degradation processes under solar light.	23
2.9	UV-Vis spectra measured for Methyl Orange through the photo-degradation process with time, the sample were taken periodically every 15 min (a-d).	23
3.1	ZnO UV-Vis spectrum measured in ethanol, after baseline correction	25
3.2	Photoluminescence spectra of synthetic non-annealed ZnO a) non-sonicated. b) sonicated. $\lambda_{EX} = 325$ nm.	26
3.3	Photoluminescence spectra for synthetic ZnO nano-particles. A) non-annealed b) annealed at 600 °C.	27
3.4	Photoluminescence spectra for ZnO nano-particles a) Synthetic non-annealed. b) Sonicated synthetic non-annealed. c) Commercial non-annealed. d) annealed at 600 °C.	28
3.5	X-ray diffraction patterns for synthetic ZnO 600 °C annealed .	29
3.6	Literature X-ray diffraction patterns of nano-particles zinc oxide (ZnO).	29
3.7	X-ray patterns 250 °C and 450 °C annealed commercial ZnO/Sand systems.	31
3.8	X-ray diffraction patterns for commercials ZnO/Clay systems annealed at 250 °C and 450 °C.	33
3.9	X-ray diffraction patterns for non-annealed and 250 °C annealed synthetic ZnO/AC system.	34

3.10	SEM images for ZnO/AC system showing ZnO flakes at porous AC..	36
3.11	Solar light photo-degradation of methyl orange (10 ppm) in 100 ml neutral mixture at room temperature under direct solar light (0.0766 W/cm^2), by different preparation methods ZnO nano-particles a) 12 hours mixing annealed at 600°C b) 5 hours mixing annealed at 600°C c) by Sonication annealed at 600°C d) 12 hours mixing non-annealed e) 5 hours mixing non-annealed.	37
3.12	UV-light Photo-degradation of methyl orange (10 ppm) under UV (0.0032 W/cm^2) at 25°C in a neutral 50 mL mixture by different preparation methods ZnO nano-particles a) 12 hours mixing annealed at 600°C b) 5 hours mixing annealed at 600°C c) by Sonication annealed at 600°C d) 12 hours mixing non-annealed e) 5 hours mixing non-annealed.	38
3.13	Effect of temperature on photo-degradation of neutral 100 mL solution methyl orange (10 ppm) using 0.20 g of 5 hours mixing ZnO at: a) 10°C b) 20°C c) 30°C d) 40°C . For better temperature control, radiation was conducted using 100 mL thermostated neutral solution of methyl orange (10 ppm) under direct solar light (Radiation Intensity 0.0634 W/cm^2) and naked ZnO (0.02g).	40
3.14	Effect of ZnO catalyst amount on rate of photo-degradation of methyl orange (100 ml solution, 10 ppm), at room temperature under neutral conditions using direct solar light (radiation intensity 0.0753 W/cm^2). ZnO Catalyst amounts were: a) 0.100g, b) 0.150 g, c) 0.200g d) 0.300g e) 0.400g .	41
3.15	Effect of contaminant concentration on photo-degradation reaction using 0.20 g ZnO in 100 mL neutral solution at room temperature under direct solar light (0.0724 W/cm^2). Methyl orange concentrations were: a) 5 ppm b) 10 ppm c) 20ppm.	42
3.16	Effect of light concentration on photo-degradation of neutral 100 mL solution methyl orange (10 ppm) using 0.20 g ZnO: a) direct solar light (Radiation	43

	Intensity 0.0597 W/cm ²). b) concentrated solar light (Radiation Intensity 0.179 W/cm ²).	
3.17	Effect of pH on rate of methyl orange degradation reaction. under UV light (0.0032 W/cm ²). All reactions were conducted at room temperature in a 50 ml solution of methyl orange (10 ppm) using 1.00g ZnO/Sand. The pH values were: a) 7 b) 9 c) 11.	54
3.18	Effect of pH on rate of methyl orange degradation reaction. under direct solar light (0.072 W/cm ²). All reactions were conducted at room temperature in a 100 ml solution of methyl orange (10 ppm) using 1.00g ZnO/Sand. The pH values were: a) 3 b) 5 c) 7 d)9 e)11	46
3.19	Effect of temperature on photo-degradation of neutral 100 mL solution methyl orange (10 ppm) using 1.00 g ZnO/Sand at: a) 10°C b) 20°C c) 30°C d) 40°C. For better temperature control, experiment were conducted in a thermostated reactor using radiation intensity 0.0753 W/cm ²	47
3.20	Effect of ZnO/Sand catalyst amount on rate of photo-degradation of methyl orange (100 ml solution, 10 ppm), at room temperature under neutral conditions using direct solar light (radiation intensity 0.0653 W/cm ²). ZnO/Sand Catalyst amounts were: a) 0.500g, b) 0.750 g, c) 1.00 g, d) 1.50 g e) 2.00 g.	48
3.21	Effect of contaminant concentration on photo-degradation reaction using 1.00 g ZnO/Sand in 100 mL neutral solution at room temperature under direct solar light (0.0739 W/cm ²). Methyl orange concentrations were: a) 5.0 ppm b) 10 ppm c) 20 ppm d) 30 ppm.	49
3.22	Effect of light concentration on photo-degradation of neutral 100 mL solution methyl orange (10 ppm) using 1.00g ZnO/Sand: a) direct solar light (Radiation Intensity 0.069 W/cm ²). b) Concentrated solar light (Radiation Intensity 0. 207 W/cm ²).	50
3.23	Effect of ZnO/Clay annealing on photo-degradation of neutral 100 mL solution methyl orange (10 ppm) using 1.00g ZnO/Clay direct solar	51

	light (Radiation Intensity 0.0737 W/cm^2). A) 250°C b) 450°C .	
3.24	Effect of temperature on photo-degradation of neutral 100 mL solution methyl orange (10 ppm) using 1.00 g ZnO/Clay at: a) 10°C b) 20°C c) 30°C d) 40°C . For better temperature control, radiation was conducted inside thermostated solution of methyl orange under direct solar light (Radiation Intensity 0.0674 W/cm^2).	52
3.25	Effect of ZnO/Clay catalyst amount on rate of photo-degradation of methyl orange (100 ml solution, 10 ppm), at room temperature under neutral conditions using direct solar light (radiation intensity 0.0597 W/cm^2). ZnO/Clay Catalyst amounts were: a) 0.50g, b) 0.75 g, c) 1.00 g, d) 1.50 g e) 2.00 g.	53
3.26	Effect of contaminant concentration on photo-degradation reaction using 1.00 g ZnO/Clay in 100 mL neutral solution at room temperature under direct solar light (0.0703 W/cm^2). Methyl orange concentrations were: a) 5 ppm b) 10 ppm c) 20 ppm d) 30 ppm.	54
3.27	Effect of light concentration on photo-degradation of neutral 100 mL solution methyl orange (10 ppm) using 1.00g ZnO/Clay: a) direct solar light (Radiation Intensity 0.0766 W/cm^2). b) Concentrated solar light (Radiation Intensity 0.2297 W/cm^2).	55
3.28	Effect of temperature on photo-degradation of neutral 100 mL solution methyl orange (50 ppm) using 0.120 g ZnO/AC at: a) 10°C b) 20°C c) 30°C d) 40°C . For better temperature control, radiation was conducted inside thermostated solution of methyl orange under direct solar light (Radiation Intensity 0.0724 W/cm^2)	57
3.29	Effect of ZnO/AC catalyst amount on rate of photo-degradation of methyl orange (100 ml solution, 50 ppm), at room temperature under neutral conditions using direct solar light (radiation intensity 0.067 W/cm^2). ZnO/AC Catalyst amounts was: a) 0.072g, b) 0.096 g, c) 0.120 g, d) 0.144 g.	58

3.30	Effect of contaminant concentration on photo-degradation reaction using 0.120g of ZnO/AC in 100 mL neutral solution at room temperature under direct solar light (0.0634 W/cm^2). Methyl orange concentrations were: a) 20 ppm b) 30 ppm c) 40 ppm d) 50 ppm.	59
3.31	Effect of light concentration on photo-degradation of neutral 100 mL solution methyl orange (50 ppm) using 0.120g of ZnO/AC: a) direct solar light (Radiation Intensity 0.067 W/cm^2). b) Concentrated solar light (Radiation Intensity 0.201 W/cm^2).	60
3.32	Figure (3.32): Effect of light concentration on photo-degradation of neutral 100 mL solution methyl orange ([1] 10 ppm, [2] 20 ppm) using ZnO thin film: a) direct solar light (Radiation Intensity 0.067 W/cm^2). b) Concentrated solar light (Radiation Intensity 0.201 W/cm^2).	61

List of Abbreviations

Symbol	Abbreviation
UV	Ultraviolet
Vis	Visible
MO	Methyl Orange
CBD	Chemical Bath Deposition
XRD	X-ray Diffraction
SEM	Scanning Electron Microscope
AC	Activated Carbon
SC	Semiconductor
e⁻	Electron
h⁺	Hole
VB	Valence Band
CB	Conduction Band
E_{bg}	Band gap
C	Contaminant concentration
T	Time
E_{act}	activation energy
pH_{zpc}	pH of zero point charge
PL	Photoluminescence
T.N.	Turnover number
Q.Y.	Quantum Yield
ppm	Part per million
λ	Wavelength
θ	Theta
Å	Angstrom
nm	Nano-meter
eV	Electron volt
w/cm²	Watt per square centimeter
hcp	Hexagonal
f	Focal length
ζ_r	photonic efficiencies
λ_{EX}	Excitation wave length

**ZnO nano-particle catalysts in contaminant degradation processes
with solar light: Naked and supported systems**

By

Hussam Ahmad Abdullah Amer

Supervisor

Prof. Hikmat Hilal

Abstract

The photo-catalytic degradation of organic contaminants (like dyes, insecticide, pesticide, ... etc) in water, air, and soil using ZnO under UV are commonly used procedures. This is due to its low costs, use of sunlight, mild reaction conditions, high photochemical reactivity, low environmental toxicity and stability to photocorrosion.

In this work commercial and synthetic nano-particles of zinc oxide and thin films were used in photodegradation of methyl orange (MO) from water under UV-light and direct solar light. $\text{ZnSO}_4 \cdot 7\text{H}_2\text{O}$ was used to prepare hexagonal ZnO nano-particles (20-25 nm) by direct precipitation method, and ZnO thin films by chemical bath deposition method. Supported ZnO onto other substances (Activating Carbon, Sand, and Clay to form ZnO/AC, ZnO/Sand, and ZnO/Clay) was also used here to enhance the contaminant photodegradation process. UV-visible scanning, photoluminescence measurements, XRD characterization, and SEM imaging were used to characterize the prepared catalyst systems. Effects of pH, catalytic concentration, contaminant concentration, temperature, and light concentration on photo-degradation rate were studied. Turnover number and Quantum yield were calculated for comparison study. Temperature effect was studied and activation energy was calculated.

Photodegradation was faster in neutral medium pH=7. Higher catalyst concentration increased photodegradation, until certain amount then showed no systematic effect. The contaminant concentration speeded up the reaction rate. Temperature showed only small effect on the rate, with only a small calculated value of activation energy. The degradation process was enhanced by concentrating solar light with concaved mirrors.

The nano-particle, thin film, and supported ZnO catalyst systems caused complete photodegradation of contaminants after enough time. The ZnO/AC system showed the highest catalyst efficiency. Pre-annealing the ZnO catalysts also enhanced the photodegradation rate.

CHAPTER 1

INTRODUCTION

1.1 Photocatalysis Overview

Since the industrial revolution, scientific and technological progress has had negative effects on the environment and the health of living organisms and humans. Therefore, there is an urgent need to reduce the impact of such negative effects, and reduce the pollution of the environment. To improve our lives scientists conducted a lot of research to find new technologies to reduce pollution risk. Most importantly, photocatalysis technology has emerged. It involves photolysis of pollutants with light using semiconductors. Examples are wide spread in water purification [1-3].

The use of titanium oxide in the photocatalytic splitting of water has been used in 1972 [1]. Since that time several studies in this area have been conducted. A variety of semiconductors have been described as photolysis catalysts for many types of organic pollutants in water under light illumination [2-3]. In the last twenty years scientists have developed many ways to understand the mechanism of photolysis [4]. Good examples of photolysis catalysts are solid metal oxides, such zinc oxide and titanium oxide. These substances have relatively high band gaps ($E_g \sim 3.0$ eV) and their conductive band edges are more positive potentials than the oxidation potentials needed for many organic contaminants.

Once a photon with energy higher than E_g is absorbed by the photocatalyst, it excites the electron from Valence Band (VB) to the Conduction Band (CB).

The corresponding photocatalytic reaction at ZnO surface can be described by the following six steps:

- (a) Adsorption of photons having an energy matches or greater than its band gap energy of ZnO.
- (b) Promotion of an electron e^- from the valence band to the conduction band generation a hole h^+ in the valence band.
- (c) e^- and h^+ diffuse and migrate to the surface where they can react.
- (d) Recombination of the electron-hole pairs.
- (e) Stabilization of e^- and h^+ at the surface to form a trapped electron and a trapped hole respectively.
- (f) Reduction of a suitable electron acceptor.

Among above reaction steps, the absorption of light (step (a)) and subsequent redox reaction at the surface (step (f)) are the key processes in photocatalysis. Steps (c) and (e) sometimes occur too fast to be observed in the reaction.

A well known mechanism for photocatalysis is shown in Figure (1.1); [2].

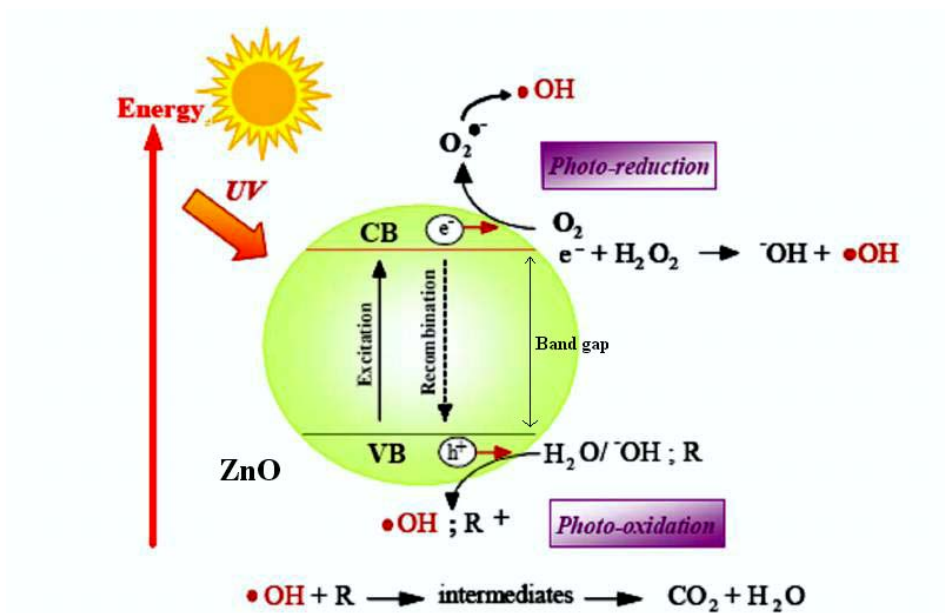


Figure (1.1): Mechanism of photo-catalysis [2].

The longest wavelength of the light source needed to excite the semiconductor depends on the value of the semiconductor band gap:

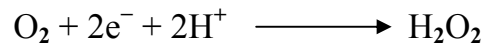
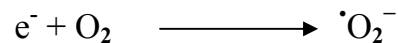
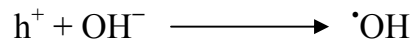
For ZnO, the value for E_g is 3.2 eV, which is equivalent to wavelength of 387 nm.

1.2 Photocatalyst Role in Contaminant Degradation

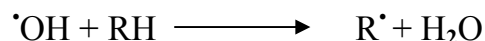
In order to excite the photocatalyst, the photon must have energy higher than the band gap. To excite zinc oxide, the wavelength of incident light should be equal or shorter than 387nm. Thus degradation of pollutants occurs in the UV region only, with wavelengths equal or shorter than 387nm. The absorbed photon energy is used in exciting the electron from the VB to the CB. Consequently, a positive hole (h⁺) is created in the VB. The electron and the hole may either recombine or separate away. Recombination may occur inside the catalyst particle or at the surface. To

our advantage, we need electron-hole separation rather than recombination. The photo excited electron-hole pairs move oppositely to the outer surface of the photocatalyst and start degradation of the adsorbed chemical species by the reaction of one or more of the transfer reactions.

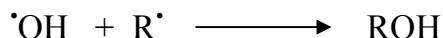
The hole can oxidize a hydroxide ion to yield a hydroxyl radical. Alternatively, the hole may react with water molecule to produce a hydroxyl radical ($\cdot\text{OH}$). The electron may react with oxygen to form a super oxide radical anion ($\cdot\text{O}_2^-$), which can further react to form hydrogen peroxide and other active oxygen radicals [5]. Both resulting free radicals are able to degrade organic contaminants into water and carbon dioxide and other minerals. The following equations explain degradation mechanism [5-7] :



The hydroxide radical reacts with organic compounds (RH) at the catalyst surface by removing the hydrogen atom on the carbon atom, and converts it to free radical (R[•]) and water by the chemical equation as follows [5-6]:



Then, the resulting radical (R[•]) reacts with the reactive oxygen radicals ([•]OH) to form hydroxy-substituted species (ROH),



Or can form tetra oxide species, which are highly unstable: [5, 7]



The resulting species releases carbon dioxide.

Finally all organic compounds can be degraded by the oxidation reaction using ZnO under solar light to carbon dioxide and water see Figure (2.8).

1.3 Why ZnO Rather Than TiO₂?

Titanium oxide (TiO₂) and zinc oxide (ZnO) have been extensively investigated as heterogeneous semiconductor photocatalysts [8–16]. This is because they offer several advantages such as, the use of oxygen as the only required oxidant and their ability to simultaneously catalyze oxidative

and reductive reactions. They also offer low cost, use of sunlight, mild reaction conditions, high photochemical reactivity, low environmental toxicity and stability to photocorrosion [17].

However, ZnO is better because it absorbs large fraction of the solar spectrum and more light quanta than TiO₂ [18]. Researchers have highlighted the performance of ZnO on degradation of some organic compounds [19-20]. In addition, ZnO has more functions than TiO₂ [21]. Recently, researchers have pointed out that ZnO can also be used in the acidic or alkaline conditions through proper treatment [22-23]. Furthermore the optimum pH reported for ZnO process is close to neutral value, whereas the optimum pH for TiO₂ mostly lies in acidic region. Hence the ZnO process is more economical for the treatment of industrial effluents.

ZnO has been reported to be more efficient than TiO₂ in some processes such as the advanced oxidation of pulp mill bleaching wastewater [24], the photooxidation of phenol [25] and photocatalysed oxidation 2-phenyl phenol [26]. In particular, ZnO has attracted much attention with respect to the degradation of various pollutants due to its high photosensitivity, stability and wide band gap. While TiO₂ is widely employed as a photocatalyst, ZnO is a suitable alternative to TiO₂ as it has a similar band gap energy (3.2 eV) [27], with larger quantum efficiency. Higher photocatalytic degradation efficiencies of contaminant dyes have been reported [28-31]. Therefore, more study on ZnO catalyst system is necessary.

1.4 ZnO Nano-Particles

The rate of photocatalytic degradation of organic pollutant depends on the size of the catalyst, crystallinity, surface morphology and the preparation methods. Nano-particles of catalyst show distinguished changes in their optical properties compared to those of bulk materials as macro size. So particle size and surface area are the effective parameters of photocatalytic activity of nano-materials. Higher reduction activity and smaller band gap energy occur for two reasons, firstly there is more radiation intensity and secondly shorter wavelengths are needed to excite electrons in nano-materials.

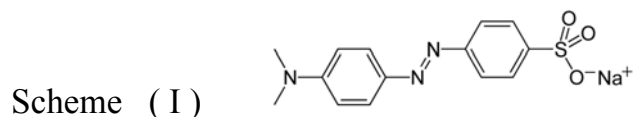
Nano-size particles absorb more radiation, due to their higher surface areas. Effect of size on the photo-degradation efficiency can be ascribed to following reasons: when the size of ZnO crystals decreases, the amount of the dispersion particles per volume in the solution will increase, resulting the enhancement of the photon absorbance, at the same time, the surface area of ZnO photocatalyst will increase, which will promote the adsorption of more dyes molecules on the surface [32].

Nano-particles also exhibit blue shift (shorter wavelengths) as the particle size is reduced [33]. Nano-sized catalysts exhibited higher reaction rates due to low mass-transfer limitations [34]. Therefore, the increased surface area of nanosized particles and high absorptivity may prove beneficial for the decomposition of dyes in aqueous media.

1.5 What's New in This Work?

Many works were done on photocatalytic degradation using TiO_2 and ZnO catalysts under solar light or UV-light. For example, CdS nano-particles sensitized TiO_2 for photo-degradation of water organic contaminants in visible irradiation [35], ZnO supported on activated carbon and sensitized with CdS for photo-degradation water organic contaminants like methyl orange and phenanzoperidine [36]. In those works naked TiO_2 and ZnO particles have been used. Recently, ZnO and TiO_2 nano-particles were prepared and used in photo-degradation of pesticide carbetamide [37], herbicide triclopyr [38], pulp milling bleaching wasterwater [39], 2-phenylphenol [40], phenol [41], reactive blue 19 [42], and acid red 14 [43]. K. Gouvea et al. confirmed that ZnO exhibits a better efficiency than TiO_2 in photocatalytic degradation of some reactive dyes in aqueous solution [44]. SiO_2 used as ZnO and TiO_2 substrate in photo-degradation process [45], PMMA [46] and PSt [47].

In this work naked and lap synthesized ZnO nano-particles were used in photo-degradation of methyl orange, the structural formula for methyl orange is shown in Scheme (I) below. Sand, clay and activated carbon are used as a substrate for both commercial and synthesized ZnO , also thin film of ZnO nano-particles were substrated on glass dishes and tested for photo-degradation efficiency.



CHAPTER 2

EXPERIMENTAL

2.1 Materials and Reagents

ZnO was purchased from Merck (Catalog no. 8849, with average particle size 230 nm). The surface area of ZnO was 47.2 m²/g. High surface area activated carbon powder 850 m²/g (Aldrich) was kindly donated by College of Engineering, ANU. Methyl orange, zinc sulfate and organic solvents (ethanol, acetone, and acetic acid) were all purchased from either Aldrich-Sigma Co. in pure form. Sand and clay were purchased from local markets and washed with concentrated hydrochloric acid then rinsed with deionized water and dried at room temperature prior to use. Zinc sulfate hepta hydrate ZnSO₄·7H₂O was purchased from Merck and was used to prepare synthetic ZnO nano-particles.

2. 2 Equipments

2.2.1 Measuring Devices

2.2.1.1 UV/ Vis Spectrophotometry

A Shimadzu UV-1601 spectro-photometer was used for electronic absorbance measurements of methyl orange concentration at wave length 480 nm.

2.2.1.2 Fluorescence Spectrometry:

A Perkin-Elmer LS50 Luminescence Spectrophotometer was used to measure emission fluorescence spectra for different catalyst systems. Emission spectra were also measured for a number of reagents. Emission spectra were used for determination of semiconductor catalyst band gap. The wavelength of the photoluminescence peak was taken to be the wavelength of the band gap for the quantum wells, as reported in literature [48].

2.2.1.3 Lux-Meter

A Lux meter (Lx-102 light meter) was used to measure the intensity of solar radiation. Values were converted to W/cm^2 using literature references [49].

2.2.1.4 Scanning Electron Microscopy (SEM)

Field emission scanning electron microscopic/energy dispersive spectroscopic (FE-SEM/EDS) studies were conducted on a Jeol Microscope, (Model JSM-6700F). The measurements were carried out in the ICMCB Laboratories, Bordeaux University, France.

2.2.1.5 X-Ray Diffraction (XRD)

XRD patterns were measured for ZnO powder and for ZnO/AC, ZnO/Clay, ZnO/Sand systems. The measurements were carried out in the ICMCB Laboratories, Bordeaux University, France, using a Philips XRD

X'PERT PRO diffractometer with Cu K α ($\lambda = 1.5418 \text{ \AA}$) as a source. The XRD lines were identified by comparing the measured diffraction patterns to JCPDS data-base cards.

2.2.2 Light Sources

Different light sources were used for photodegradation of organic pollutants like: direct sun light, concentrated sun light (by Mirrors), and UV Lamps.

2.2.2.1 Direct Sun Light

Direct sun light was used for photodegradation experiment with nano-particle ZnO powder, ZnO/AC, ZnO/Clay and ZnO/Sand systems.

2.2.2.2 Concentrated Sun Light (by Mirrors)

Sun light was concentrated by two concave mirrors with 18 cm diameter and focal length (f) equal 50 cm.

2.2.2.3 UV Lamp

Photo-degradation reactions were conducted in a magnetically stirred double-walled condenser cell equipped with a thermostated water flow. The reactor walls were covered with aluminum foil to reflect astray light and to protect persons from the harmful UV-light. The source of light was adjusted above the reactor cell at a suitable height (Figure 2.1) Lamp.

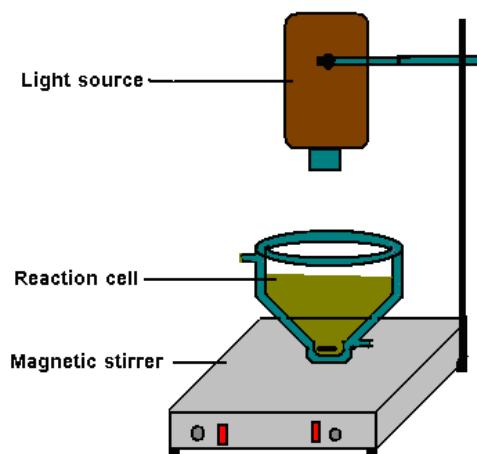


Figure (2.1): Arrangement of photocatalytic reactor.

Illumination in the UV range was carried out using a 300 W/ 230V mercury tungsten (Osram Ultra-Vitalux) lamp housed in a protection box with luminance (4400 lux, $0.000644217 \text{ W/cm}^2$). Table (1) summarizes the features of the used UV lamp. Its spectrum, is shown in Figure (2.2) in comparison with solar light and halogen spot lamp spectra.

Table (1): UV lamp specifications [50].

Model	Lifespan (hours)	Rated Wattage (W)	Lamp Voltage (V)	Light Technical Data
003313	1000	300	230	UVA radiated power 315...400 nm, 13.6W UVB radiated power 280..315 nm, 3.0W

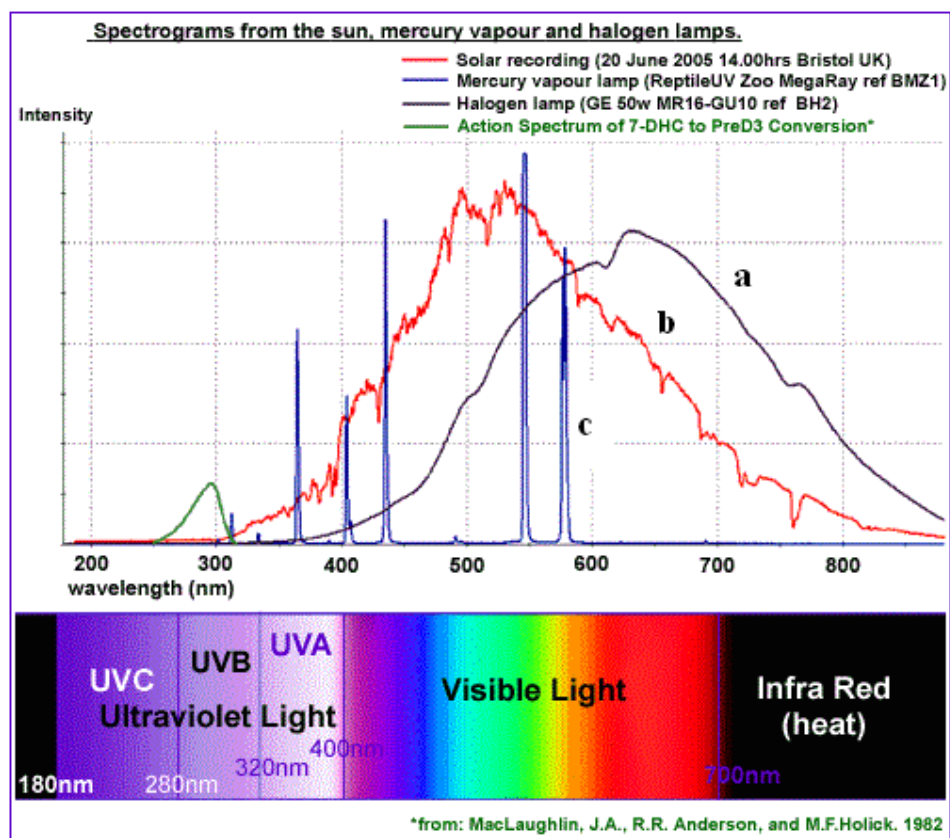


Figure (2.2): Spectrograms for: a) halogen lamps b) sun light c) mercury vapor lamp [51]

2.3 Solution Preparation

The following solutions were prepared and used:

- Sodium hydroxide solution (NaOH, 0.20 M) was prepared by dissolving 4.00 g of NaOH in distilled water and was then diluting to 0.50 liter.
- Sodium hydroxide solution (NaOH, 0.50 M) was prepared by dissolving 10.00 g of NaOH in distilled water and was then diluting to 0.50 liter.
- Hydrochloric acid solution (HCl, 0.20 M) was prepared by diluting 10.50 ml of 32% HCl to 0.50 liter with distilled water.

- Stock methyl orange solution: 0.10g of methyl orange was dissolved in hot deionized distilled water. The solution was then diluted to 1.00 liter to make the final concentration 100 ppm ($3 \times 10^{-4} \text{M}$). Different diluted solutions (50, 30, 20, 15, 10, and 5 ppm) were then prepared from the stock solution.
- Zinc sulfate solution (100 ppm)($1.53 \times 10^{-3} \text{M}$) was prepared by dissolving 0.4395 g of $\text{ZnSO}_4 \cdot 7\text{H}_2\text{O}$ (m.wt = 287.53 g/mol) in distilled water and was then diluting to 1.00 liter.
- Zinc sulfate solution ($1.88 \times 10^{-3} \text{M}$) was prepared by dissolving 5.4056 g of $\text{ZnSO}_4 \cdot 7\text{H}_2\text{O}$ in distilled water and was then diluting to 1.00 liter.
- Ethylenediamine solution ($30 \times 10^{-3} \text{M}$) was prepared by diluting 2.006 ml of ethylenediamine to 1.00 liter with distilled water.

2.4 Materials Preparation Techniques

In this work different techniques were used to prepare different types of ZnO (thin films, nano particles, and ZnO/AC, ZnO/Clay, ZnO/Sand, systems).

2.4.1 ZnO Thin Films on Glass

Thin films of ZnO were prepared on glass substrate by chemical bath deposition technique (CBD). After scrubbing with soap, the substrates were rinsed in running deionized water. The optimum CBD conditions for

achieving structured but adherent ZnO films have been previously described [52].

Appropriate amounts of zinc sulfate $\text{ZnSO}_4 \cdot 7\text{H}_2\text{O}$ (0.0188 M) and ethylenediamine (0.03 M) were mixed. The pH of the bath was raised by addition of base (0.5 M, NaOH). The solution was maintained at a temperature of $60^\circ\text{C} < T < 65^\circ\text{C}$, while the bath was continuously stirred. [53]. Thin ZnO films on glass are shown in Figure (2.3) below:



Figure (2.3): ZnO thin films on glass

2.4.2 ZnO Nano Particles

Nano particles of ZnO were synthesized by two ways, Firstly by magnet bar stirring without Sonication, and secondly by Sonication without magnet bar stirring.

2.4.2.1 Preparation by Sonication

In this work ZnO nanocrystalline particles were prepared using the precipitation method. $\text{ZnSO}_4 \cdot 7\text{H}_2\text{O}$ was used as the starting material and NaOH as precipitant without further purification. The resulting slurry was continuously sonicated for 5 and 12 hour, and then washed with deionized water. The wet powder was dried to form the precursor of ZnO. Finally, the precursor was calcined in air at 600°C to produce the nanosized ZnO photocatalyst as shown in Figure (2.4):



Figure (2.4): Sonication process for nanocrystalline ZnO preparation

2.4.2.2 Preparation Without Sonication

In this work ZnO nanocrystalline particles were prepared using the precipitation method. $\text{ZnSO}_4 \cdot 7\text{H}_2\text{O}$ was used as the starting material and NaOH as precipitant without further purification. The resulting slurry was continuously stirred for 5 and 12 h, and then washed with deionized water. The wet powder was dried to form the precursor of ZnO as shown in Figure (2.5). Finally, the precursor was calcined in air at 600°C to produce the ZnO nanosized photocatalyst [54].

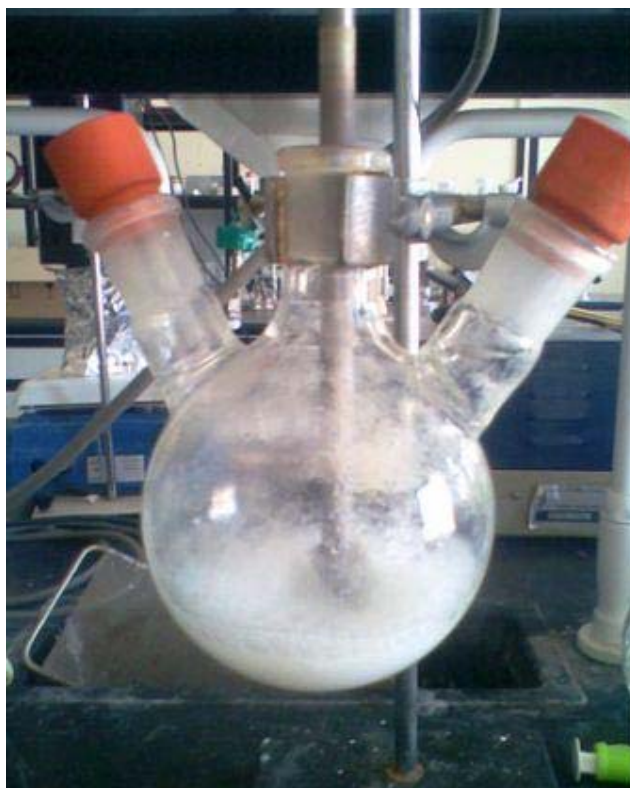


Figure (2.5): Precipitation method for nanocrystalline ZnO preparation

2.4.3 ZnO/AC

Synthesized and commercial ZnO (15.00 g) was mechanically stirred with AC (3.00 g) in aqueous solution with heating to evaporate maximum amount of water for 40 minutes in the dark. The resulting ZnO/AC was filtered and dried at room temperature as shown in Figure (2.6). Some ZnO/AC was calcinated at 200⁰C to study the annealing effects.



Figure (2.6) Precipitation method for nanocrystalline ZnO/AC preparation

2.4.4 ZnO/Clay

Commercial ZnO (3.00 g) was mechanically stirred with precleaned white Clay (12.00 g) granules in aqueous solution for 1 hour and heated to evaporate maximum amount of water. The resulting ZnO/Clay was dried at room temperature. It was calcinated at 250 °C and 450 °C to study annealing effect. It was then stored at room temperature.

2.4.5 ZnO/Sand

ZnO/Sand was prepared in a similar manner to ZnO/Clay. Commercial ZnO (3.00 g) was mechanically stirred with precleaned white Sand granules (12.00 g) in aqueous solution for 1 hour and heated to evaporate maximum amount of water. The resulting ZnO/Sand was dried at room temperature. It was calcinated at 250 °C and 450 °C to study annealing effect. It was then stored at room temperature.

2.4.6 Annealing

Annealing was conducted under air using a thermo-stated horizontal tube furnace. The prepared and commercial ZnO systems were inserted in the middle of a long Pyrex cylinder. The heat was raised to (250 and 450) °C for ZnO/Clay, and ZnO/Sand systems. The ZnO/AC system was annealed at 200 °C, where as the synthetic zinc oxide was annealed at 600 °C. All samples were annealed for 20 min before being allowed to cool at room temperature.

2.5 Catalytic Experiment

Control degradation experiments were conducted with no catalyst under direct sun light. Other experiments were conducted in the presence of a catalyst in the dark. In these experiments contaminant concentration did not change after 40 minutes. In the presence of ZnO/AC or ZnO/Clay in the dark, the concentration of contaminant significantly changed after 40 minutes, indicating adsorption of contaminant onto activated carbon or Clay surfaces.

In the presence of sand, contaminant concentration did not change so there was no adsorption by sand. This is due to relatively low surface area of sand. Figure (2.7) shows remaining concentration of contaminants with time under control experiments.

For ZnO/Clay, ZnO/AC systems a known amount of the solid was placed in the reactor in which aliquot of pollutant solution of known concentration was added. The stirred was mixed for 40 minutes in the dark in order to reach the absorption equilibrium.

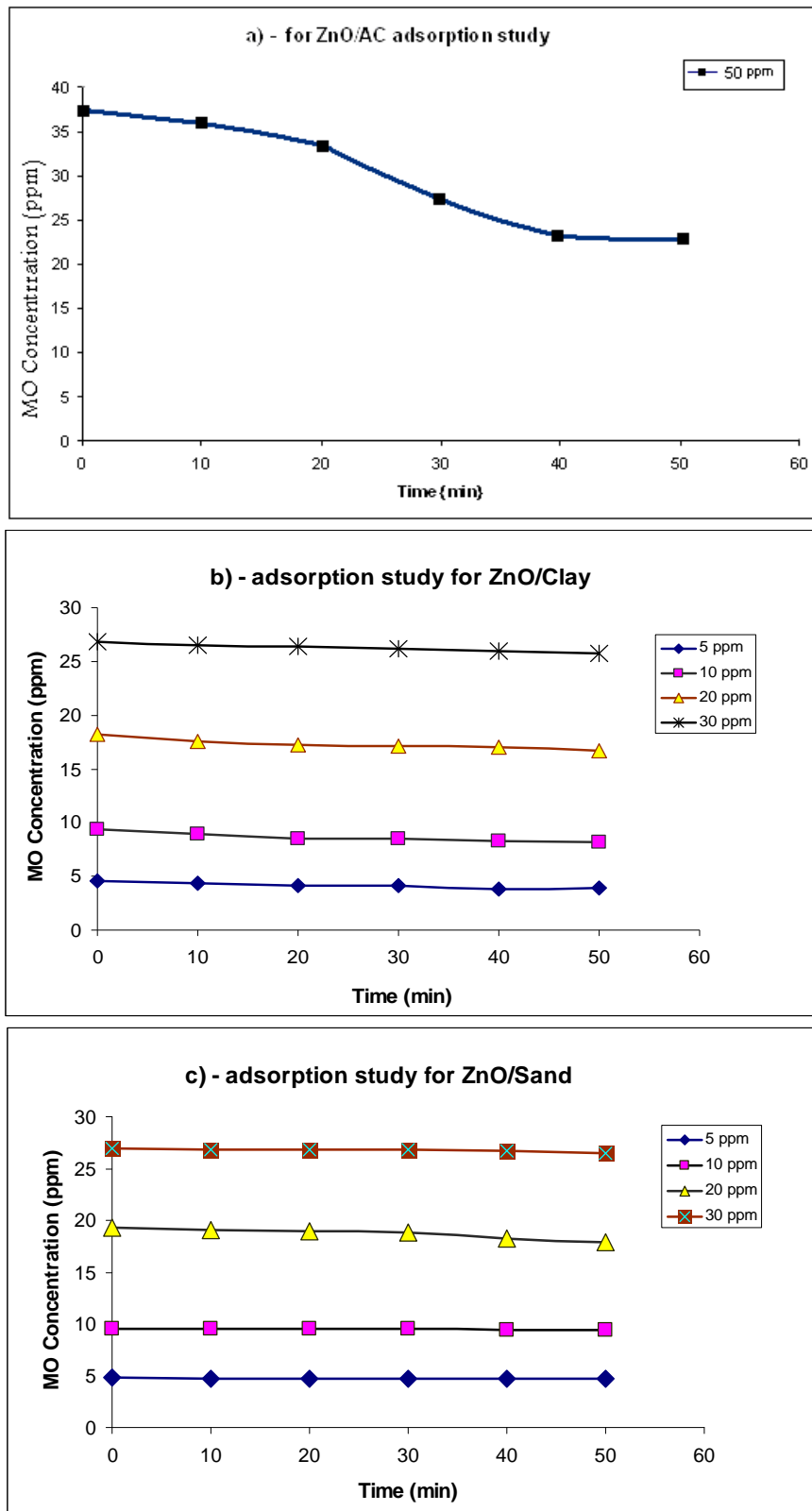


Figure (2.7): Adsorption of contaminant on a) ZnO/AC b) ZnO/Clay c) ZnO/Sand, in the dark.

The catalyst system ZnO powder, ZnO/Sand or ZnO/Clay was then added to 100 ml of pollutant aqueous solution with a known concentration. The photo-degradation reaction was investigated using UV lamp, a direct or concentrated solar light using a concentrating mirror, Figure (2.8). The incident solar radiation was measured with a lux-meter. The sunlight intensity at the beginning and end of the experiment was measured. The main daily temperature was 35⁰C.

Aliquots (5 ml) were withdrawn from the pollutant solution at various time intervals for analysis. Each sample was centrifuged at 5000 rev/min for 5 minutes.

A spectro-photometer was used to measure remaining methyl orange in the sample complete mineralization of either contaminant after reaction completion was confirmed by the absence of 480 nm absorption for Methyl Orange, Figure (2.9). The absence of any benzene derivatives was also confirmed by the absence of any absorption bands characteristics for phenyl group at 200 nm or longer, as observed from absorption spectra after reaction completion. Aqueous solutions with different nominal methyl orange concentrations: 5 ppm, 10 ppm, 15 ppm, 20 ppm, 30 ppm, 50 ppm were prepared. An absorbance vs. concentration calibration curve was used to analyze remaining methyl orange through out the course of degradation reaction.



Figure (2.8) ZnO degradation processes under solar light.

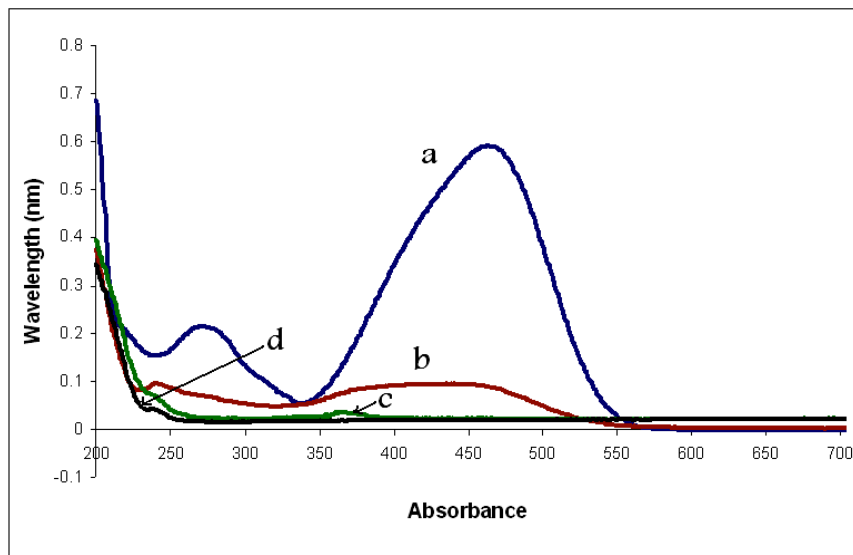


Figure (2.9) UV-Vis spectra measured for Methyl Orange through the photo-degradation process with time, the sample were taken periodically every 15 min (a-d).

CHAPTER 3

RESULTS

3.1 Catalyst System Characterization

3.1.1 ZnO Nano-Particles Annealed and Non-Annealed

Different characterization methods were used to characterize the synthetic ZnO nano-materials such as: Electronic Absorption Spectra, PL Emission, X-Ray Diffraction and SEM.

3.1.1.1 Absorption Spectra

The prepared catalyst was characterized using UV-Visible spectrophotometry. The baselines were measured for pure ethanol solution. The spectra were then scanned on dispersed small amount of fine solid catalyst particles in ethanol inside a quartz analysis cell in the UV-Visible range. The spectra are shown in Figure (3.1). A maximum at ~390 nm due to ZnO was observed.

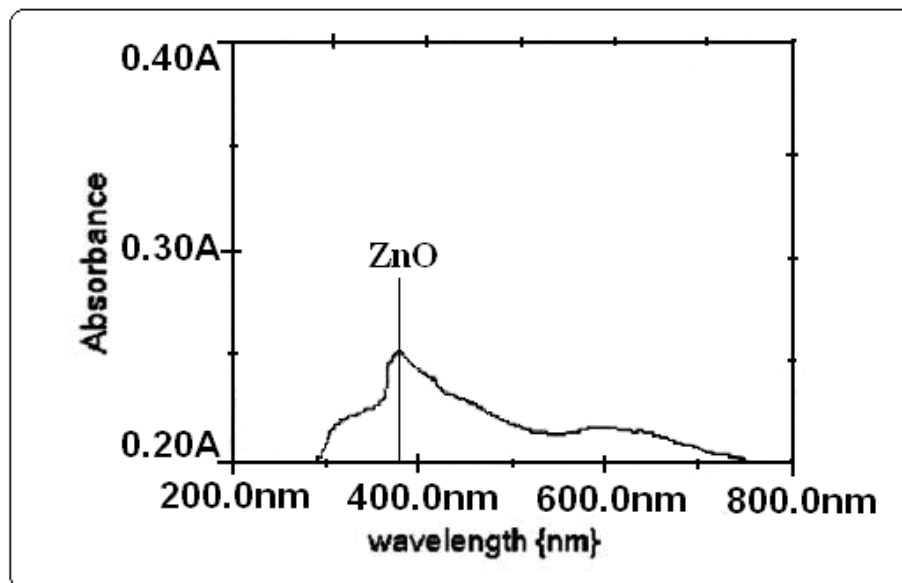


Figure (3.1): ZnO UV-Vis spectrum measured in ethanol, after baseline correction.

3.1.1.2 Photoluminescence Emission Spectra

Fluorescence Emission spectra were used to measure semiconductor catalyst band gap. The wavelength of the photoluminescence peak was taken to be the wavelength of the band gap for the quantum wells, as reported in literature . The spectrum exhibits two emission peaks, one is located at around 392 nm (UV region) corresponding to the near band gap excitonic emission and the other is located at around 520 nm, and 450 nm attributed to the presence of singly ionized oxygen vacancies. The emission is caused by the radiative recombination of a photogenerated hole with an electron occupying the oxygen vacancy [48]. A small amount of the catalyst powder was dispersed in ethanol, and placed in the analysis quartz cell. The sample was excited at a proposed wavelength. Emission spectrum was then measured.

Photoluminescence emission spectra were measured for both the sonicated and non-sonicated synthetic hexagonal ZnO nano-particles. The excitation wavelength was 325 nm. The emission peaks were at ~ 390 nm for the sonicated synthetic ZnO and ~ 395 nm for non-sonicated synthetic ZnO nano-particles (Figure 3.2).

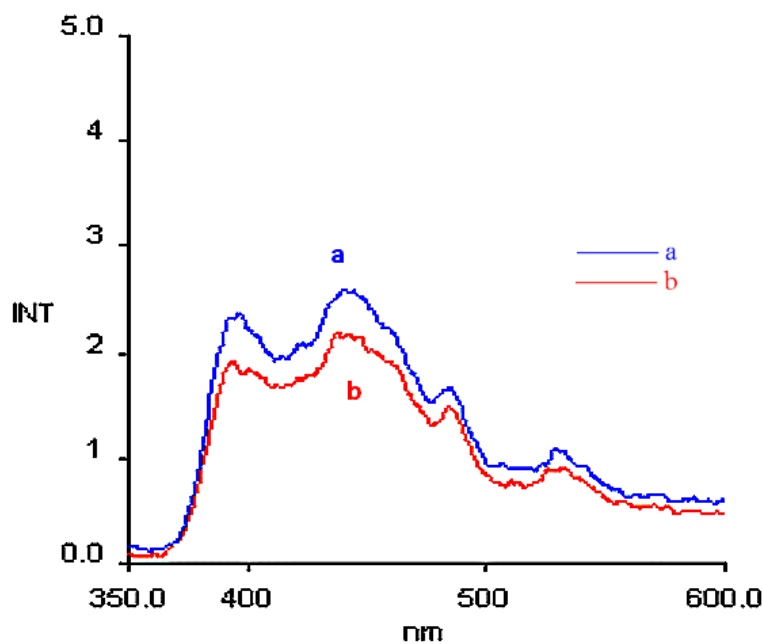


Figure (3.2): Photoluminescence spectra of synthetic non-annealed ZnO a) non-sonicated. b) sonicated. $\lambda_{\text{EX}} = 325$ nm.

Emission spectra were also measured for both pre-annealed (at 600°C) and non-annealed synthetic ZnO. The pre-annealed ZnO showed emission wavelength at ~ 397 nm, and the non-annealed ZnO showed emission at ~ 395 nm, as shown in (Figure 3.3).

For more comparison purposes photoluminescence spectra are collectively shown in (Figure 3.4) for synthetic and commercial ZnO (annealed and non-annealed).

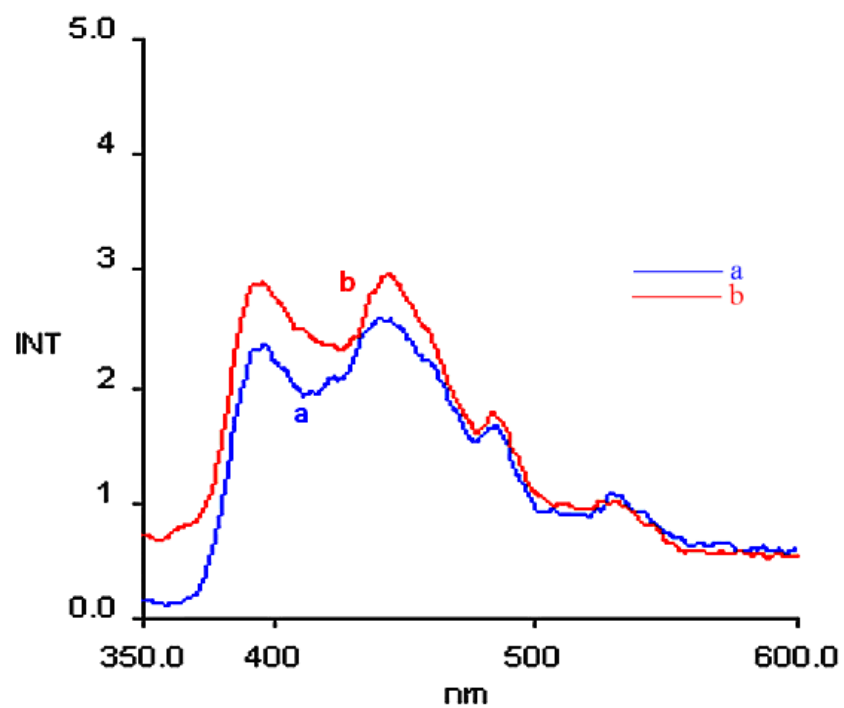


Figure (3.3): Photoluminescence spectra of synthetic ZnO nano-particles a) non-annealed b) annealed at 600 °C

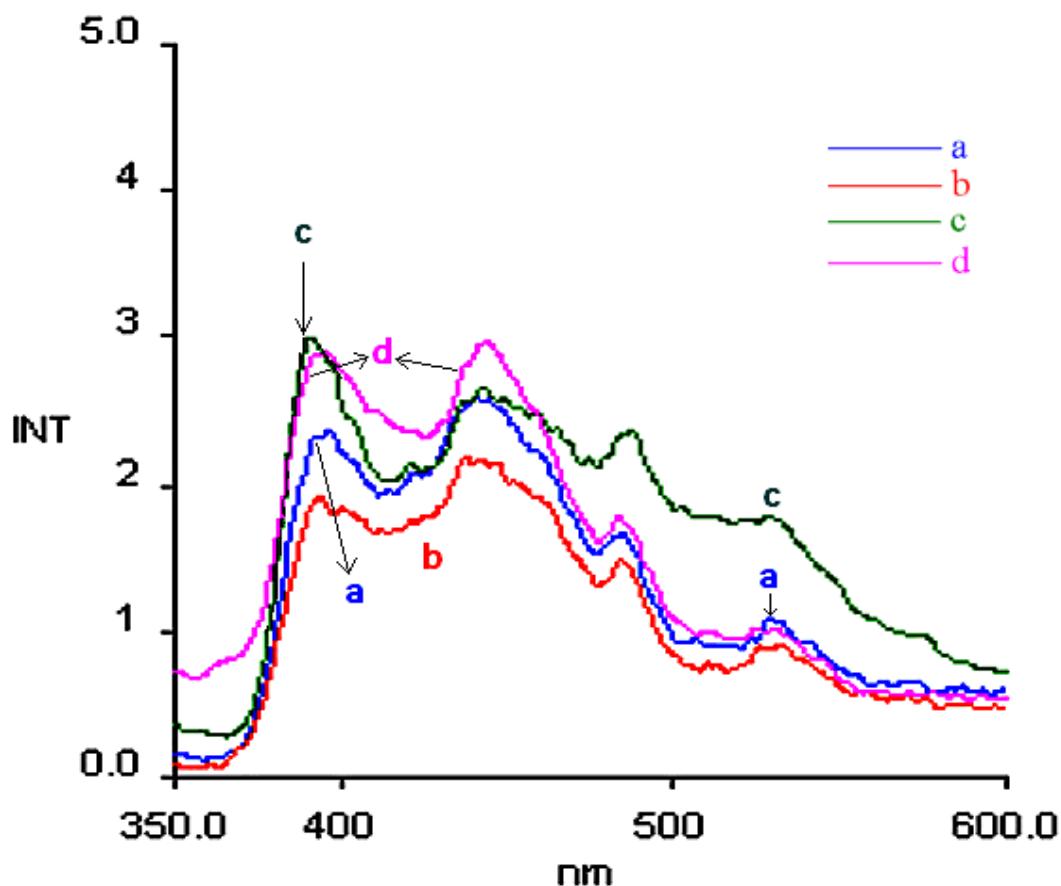


Figure (3.4): Photoluminescence spectra of ZnO nano-particles a) Synthetic non-annealed. b) Sonicated synthetic non-annealed. c) Commercial non-annealed. d) Synthetic annealed at 600 °C

3.1.1.3 X-ray Diffraction (XRD):

The X-Ray Diffraction patterns were measured for all prepared ZnO systems. The XRD pattern showed noticeable peaks for non-annealed synthetic ZnO (sonicated and non-sonicated) at 2θ values of 32.1 (100), 34.8 (002), 36.6 (101), 47.9 (102), 56.9 (110) and 63.1 (103). For the 600 °C annealed system, patterns of 2θ values 31.8 (100), 34.6 (002), 36.3 (101), 47.6 (102), 56.7 (110) and 63.0 (103) were obtained, Figure (3.5). The X-

ray patterns show hexagonal crystal type for ZnO. The results coincide with literature XRD pattern for hexagonal wurtzite ZnO, Figure (3.6), [55].

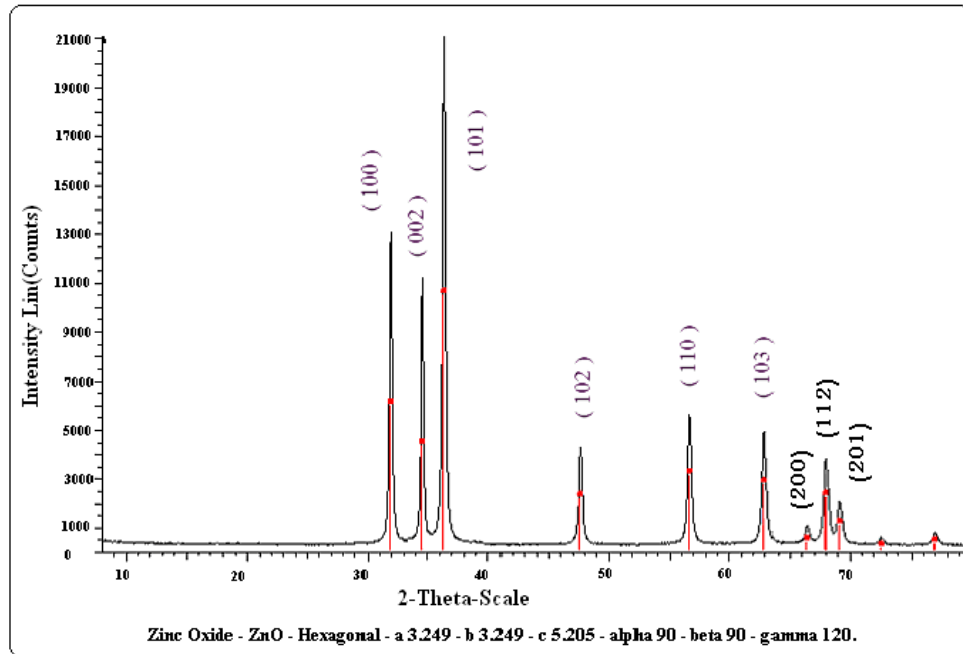


Figure (3.5): X-ray diffraction patterns for synthetic ZnO 600 °C annealed

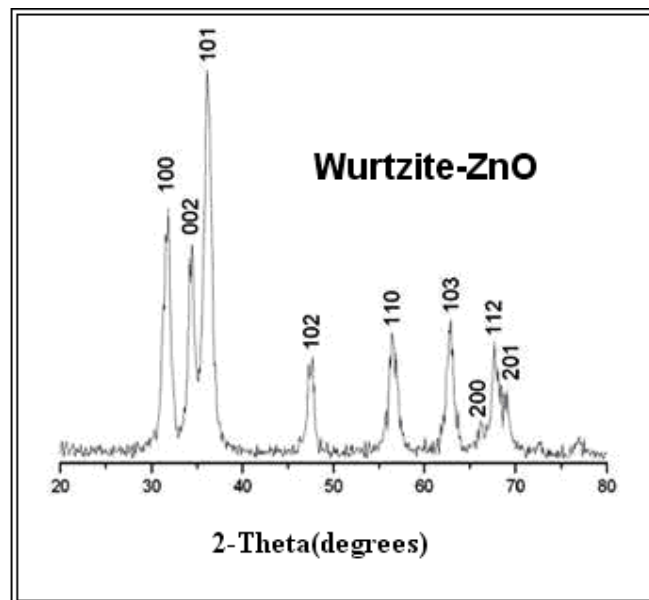


Figure (3.6): Literature X-ray diffraction patterns for ZnO nano-particles, [55].

Particle size was calculated using the Scherrer equation:

$$D = (0.9\lambda) / (b \cos \theta)$$

Where **D** is the average crystallite diameter (nm), λ is the X-ray wavelength (nm), **b** is the full width at half maximum (FWHM) of the peak corrected for instrumental broadening (rad.) and θ is the Bragg's angle (deg.). The calculated ZnO average particle diameters for non-annealed and pre-annealed ZnO nano-particles were 21.8 and 24.0 nm respectively. Little crystallite growth by annealing at 600°C is observed from measured particle sizes. This is in agreement with absorption and emission spectral results.

Table (2): Peak position and particle size values for different synthetic ZnO systems .

ZnO Type	Peak position (2 θ) deg.	ZnO crystal Type	average particle diameters D (nm) D=(0.9 λ)/(FWHM COS θ) $\lambda = 0.154$ nm
Non-annealed sonicated	32.1, 34.8, 36.6, 47.9, 56.9, and 63.1	Hexagonal	21.8 nm
Non-annealed	32.1, 34.8, 36.6, 47.9, 56.9, and 63.1	Hexagonal	21.8 nm
Annealed at 600°C	31.8, 34.6, 36.3, 47.6, 56.7, and 63.0	Hexagonal	24.0 nm

3.1.2 Sand-Supported ZnO System

3.1.2.1 X-ray Diffraction (XRD):

The X-Ray Diffraction patterns were measured for commercial ZnO systems supported onto sand. The XRD pattern showed noticeable peaks for 250 °C annealed ZnO/Sand systems at 2θ values of 32.1 (100), 34.7 (002), 36.6 (101), 47.8 (102), 56.9 (110), and 63.1 (103). For the 450 °C annealed system, patterns of 2θ values 32 (100), 34.7 (002), 36.5 (101), 47.8 (102), 56.8 (110), and 63.1 (103) are shown in Figure (3.7). The X-ray patterns show a hexagonal crystal type for ZnO. Peaks for SiO₂ that present hexagonal Quartz at 2θ values of 21.0, 26.7, and 45.9 are also observed.

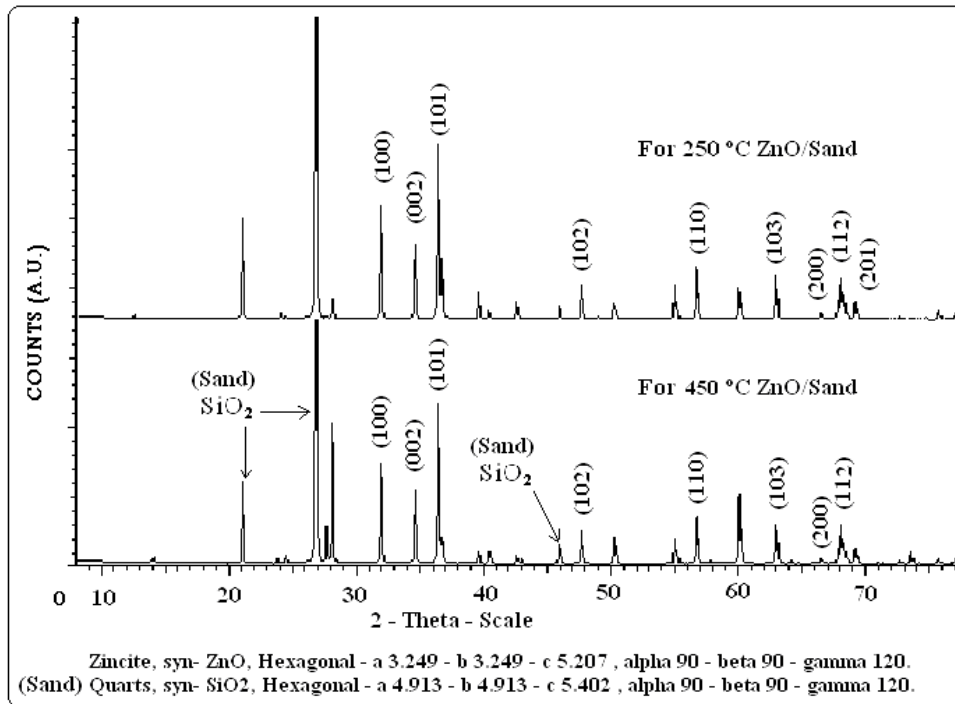


Figure (3.7):X-ray patterns 250 °C and 450 °C annealed commercial ZnO/Sand systems.

Particle size was calculated using the Scherrer equation where the calculated ZnO average particle diameters for commercial ZnO/Sand systems annealed at 250 °C and 450 °C were 19.7 and 25.21 nm respectively.

3.1.3 Clay-Supported ZnO System

3.1.3.1 X-ray Diffraction (XRD):

The X-Ray Diffraction patterns were measured for commercial ZnO systems supported onto clay. The XRD pattern showed noticeable peaks for 250 °C annealed ZnO/Clay systems at 2θ values of 31.9 (100), 34.6 (002), 36.4 (101), 47.7 (102), 56.7 (110), and 63. For the 450 °C annealed system, patterns of 2θ values 32 (100), 34.7 (002), 36.5 (101), 47.8 (102), 56.8 (110), and 63.1 (103) were observed, Figure (3.10). The X-ray patterns show a hexagonal crystal type for ZnO. Peaks for Feldspar (K-component) $K(\text{AlSi}_3\text{O}_8)$ were also observed at 2θ values of 21.1, 27.0, 30.0 and 42.8, Figure (3.8).

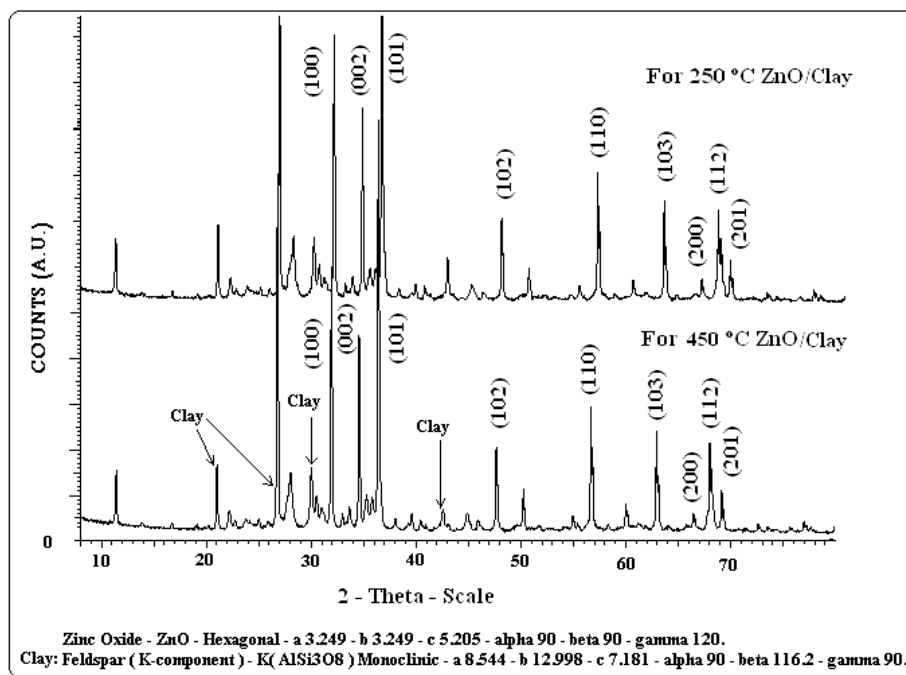


Figure (3.8): X-ray diffraction patterns for commercial ZnO/Clay systems annealed at 250 °C, and 450 °C.

Particle size were calculated using the Scherrer equation where the calculated ZnO average particle diameters for commercial ZnO/Clay systems annealed at 250 °C and 450 °C were 24.06 and 25.21 nm respectively.

3.1.4 AC-Supported ZnO System Annealed and Non-Annealed

3.1.4.1 X-ray Diffraction (XRD):

The X-Ray Diffraction patterns were measured for synthetic ZnO systems supported onto activated carbon. The XRD pattern showed noticeable peaks for non-annealed ZnO/AC systems at 2θ values of 32 (100), 34.6 (002), 36.5 (101), 47.7 (102), 56.8 (110), and 63 (103) Figure (3.11). For the 200 °C annealed system, patterns of 2θ values 31.9 (100),

34.6 (002), 36.4 (101), 47.7 (102), 56.8 (110), and 63 (103) were observed. The X-ray patterns show a hexagonal crystal type for ZnO. A small peak at $2\theta = 44.6$ emerged corresponding to AC, Figure (3.11).

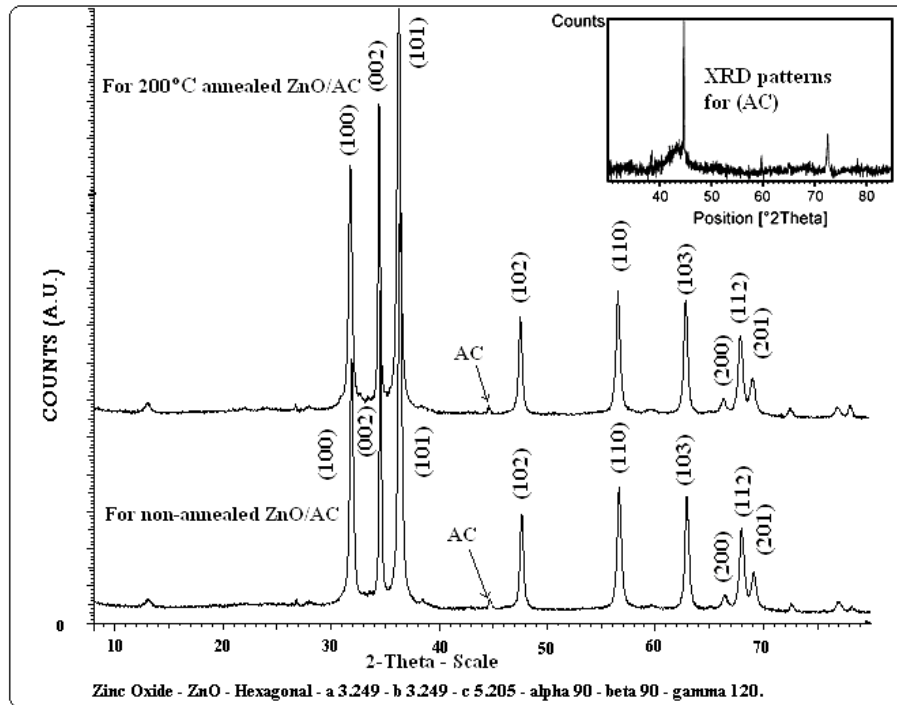


Figure (3.9): X-ray diffraction patterns for non-annealed and 250 °C annealed synthetic ZnO/AC system.

Particle size was calculated using the Scherrer equation. The calculated ZnO average particle diameters for synthetic ZnO/AC systems for non-annealed and annealed at 200 °C were 20.8 and 23.0 nm respectively.

3.1.4.2 Scanning Electron Microscopy (SEM)

Field emission scanning electron microscopic/energy dispersive spectroscopic (FE-SEM/EDS) studies were conducted on a Jeol microscope, (Model JSM-6700F). SEM scanning was performed to

investigate the surface morphology of the ZnO/AC particles. Surface morphology of the ZnO particles over Activated carbon is depicted in Figure (3.10). SEM image shows that the ZnO exists as nano-particles of agglomeration flakes with uniform nano-scale thicknesses and random length and orientations. The nano-particles are attached to the Activated carbon surfaces. The estimated ZnO nano-particle thickness is about ~20 nm. This is evident from size 1 μ m scale pictures.

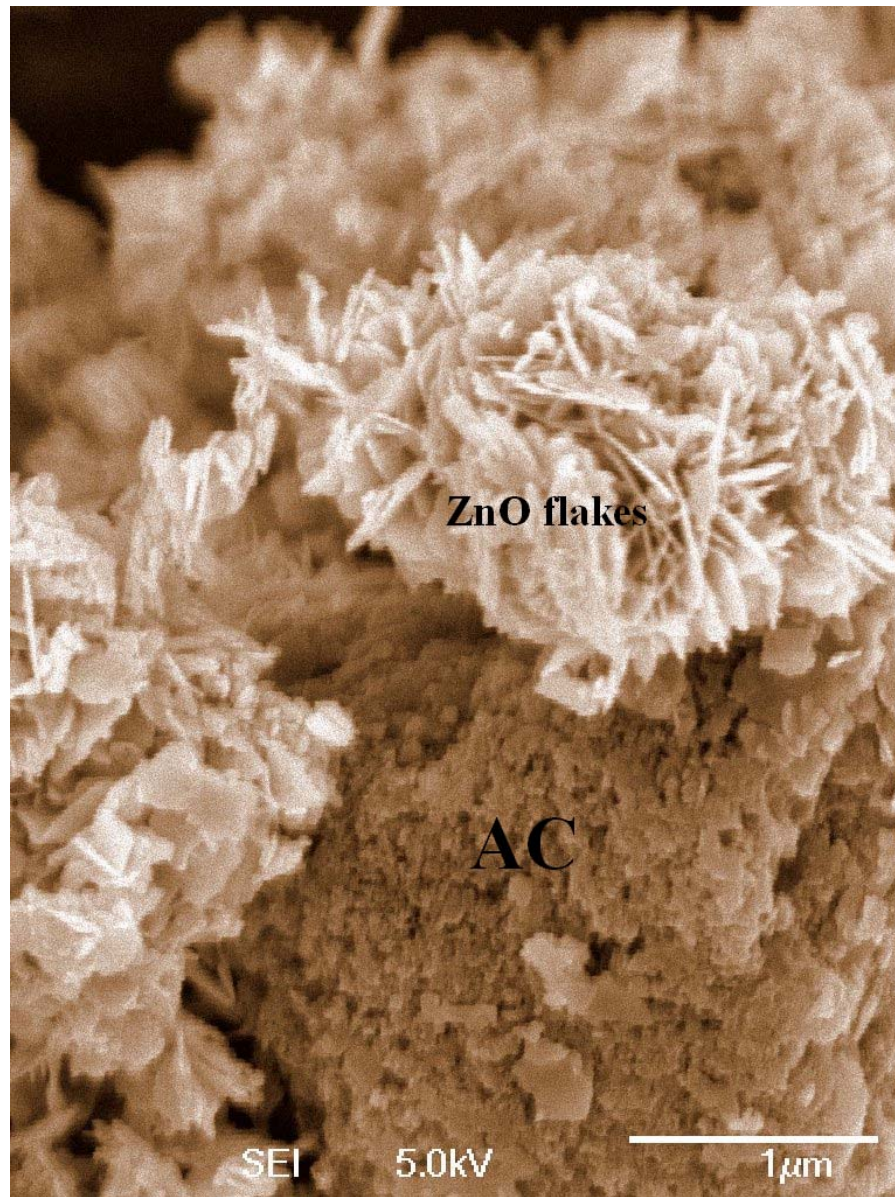


Figure (3.10): SEM images for ZnO/AC system showing ZnO flakes at porous AC.

3.2 Photodegradation Reactions

3.2.1 ZnO Nano-Particles (Annealed and Non-Annealed)

ZnO nano-particles prepared by different methods were used for photodegradation of neutral 10 ppm methyl orange solution under direct solar light (Figure 3.11) and under UV-light (Figure 3.12). The figures

show values of remaining contaminant methyl orange concentration measured with time.

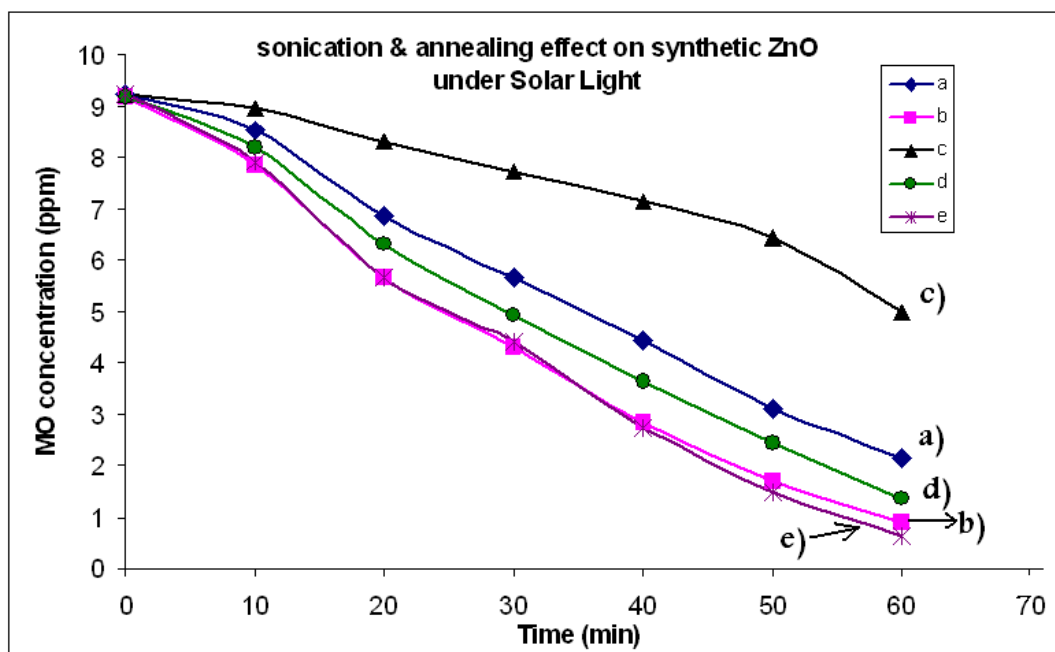


Figure (3.11): Solar light photodegradation of methyl orange (10 ppm) in 100 ml neutral mixture at room temperature under direct solar light (0.0766 W/cm^2), by different preparation methods ZnO nano-particles a) 12 hours mixing annealed at $600 \text{ }^\circ\text{C}$ b) 5 hours mixing annealed at $600 \text{ }^\circ\text{C}$ c) by sonication annealed at $600 \text{ }^\circ\text{C}$ d) 12 hours mixing non-annealed e) 5 hours mixing non annealed.

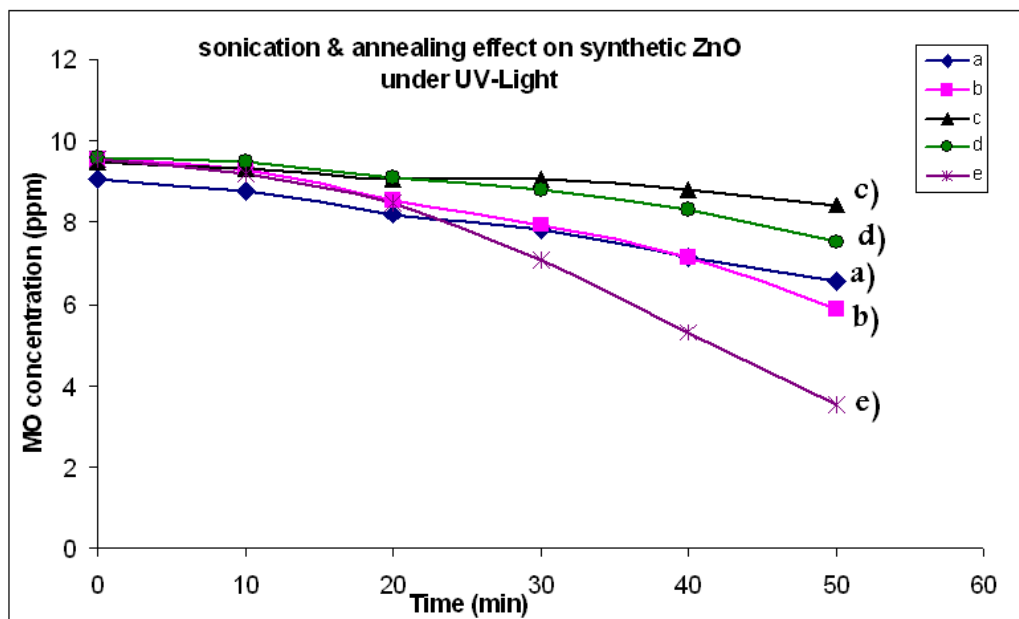


Figure (3.12): UV-light Photodegradation of methyl orange (10 ppm) under UV (0.0032 W/cm^2) at 25°C in a neutral 50 mL mixture by different preparation methods ZnO nanoparticles a) 12 hours mixing annealed at 600°C b) 5 hours mixing annealed at 600°C c) by sonication annealed at 600°C d) 12 hours mixing non-annealed e) 5 hours mixing non-annealed.

Turnover number of a heterogeneous photocatalyst, (T.N.), is the number of photogenerated transformations with respect to the number of active sites of the heterogeneous photocatalyst that is known.

Quantum yield of a photocatalytic process, (Q.Y.), is the number of molecules of a given product formed (alternatively, of a given reactant consumed) per photon of incident light at a given wavelength:

$$\text{Q.Y} = (\text{number of reacted molecules})/(\text{number of incident photons})$$

Turnover number (T.N.) and quantum yield (Q.Y.) values were calculated after 40 minutes for each catalyst system as shown in Table (3).

Table (3): Values of T.N. and Q.Y. for MO degradation using different catalyst systems, after 40 min.

System	Under solar light		Under UV-light	
	T.N.	Q.Y.	T.N.	Q.Y.
a) 12 hour mixing annealed at 600 °C	0.00278	0.000408	0.00143	0.00501
b) 5 hour mixing annealed at 600 °C	0.00359	0.000526	0.00163	0.00502
c) Sonication annealed at 600 °C	0.00120	0.000175	0.00600	0.02108
d) 12 hour mixing non-annealed	0.00320	0.000468	0.00850	0.00297
e) 5 hour mixing non-annealed	0.00363	0.000533	0.00235	0.00825

From Table (3) and Figures (3.11 and 3.12) the photodegradation of methyl orange under solar light is better than under UV lamp light. Turnover number values under solar light are greater than under UV lamp light. The Q.Y. values were lower under solar light for all systems except sonicated ones. For each plot we note that annealing at high temperatures (600°C) causes slight increase in reaction rate where turnover number and quantum yield values slightly increased as shown in Table (3). On the other hand the results show that the five hour mixing are the best methods for ZnO preparation. The sonication method is not the favorite choice, where the turnover number and quantum yield values are the highest for five hours mixing method and the lowest for sonicated one.

3.2.1.1 Effect of Temperature

The effect of temperature on the rate of MO degradation using 0.20g nano particles of ZnO was studied within the used temperature range (10-40 °C), Figure (3.13). Turnover number (and quantum yield) values calculated after

40 minutes at different temperature (10, 20, 30, and 40 °C) were: 0.00175 (30.91×10^{-5}), 0.00143 (25.34×10^{-5}), 0.0025 (44.29×10^{-5}) and 0.00282 (49.88×10^{-5}) respectively. The T.N. and Q.Y. values indicate that there was very little difference in rates between experiments calculated at different temperatures. Increasing the temperature showed no significant effect on the reaction rate. The value of activation energy was measured for the reaction process, using Arrhenius method The value was only 9.0 KJ/mol.

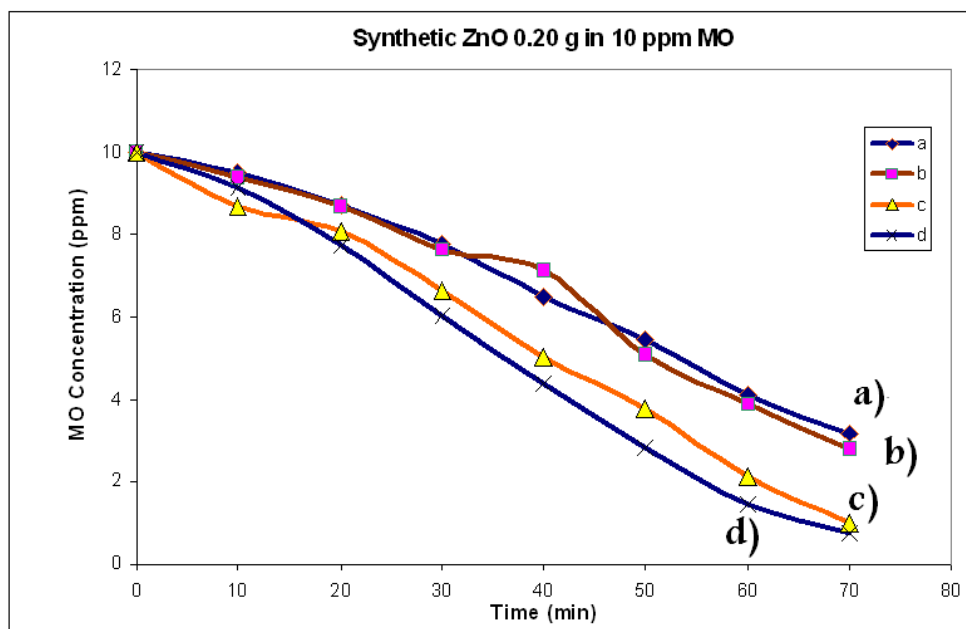


Figure (3.13): Effect of temperature on photo-degradation of neutral 100 mL solution methyl orange (10 ppm) using 0.20 g 5 hours mixing ZnO at: a) 10°C b) 20°C c) 30°C d) 40°C. For better temperature control, radiation was conducted using 100 mL thermostated neutral solution of methyl orange (10 ppm) under direct solar light (Radiation Intensity 0.0634 W/cm²) and naked ZnO (0.20 g).

3.2.1.2 Effect of Catalyst Concentration

The effect of concentration of ZnO on photo-degradation of MO was investigated. Different amount of catalyst in the range 0.10 to 0.40 g/100 ml were used. Figure (3.14) shows reaction profiles for different catalyst amounts.

Turnover number (and quantum yield) values calculated after 40 minutes for (0.10, 0.15, 0.20, 0.30, and 0.40)g values were: 0.450×10^{-3} (0.0671×10^{-3}), 1.645×10^{-3} (0.2454×10^{-3}), 2.035×10^{-3} (0.3036×10^{-3}), 2.595×10^{-3} (0.3872×10^{-3}) and 1.995×10^{-3} (0.4468×10^{-3}) respectively. The increasing on T.N. and Q.Y. values indicate that the rate increases with increasing ZnO amount, to a certain limit. This indicates screening effect by ZnO particles.

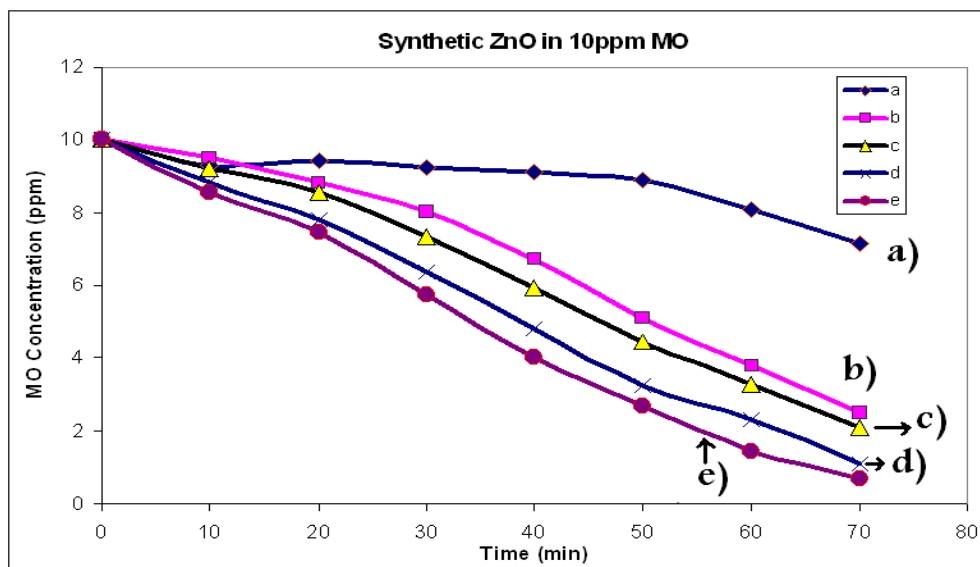


Figure (3.14): Effect of ZnO catalyst amount on rate of photo-degradation of methyl orange (100 ml solution, 10 ppm), at room temperature under neutral conditions using direct solar light (radiation intensity 0.0753 W/cm^2). ZnO Catalyst amounts were: a) 0.100g, b) 0.150 g, c) 0.200g d) 0.300g e) 0.400g.

3.2.1.3 Effect of Contaminant Concentration

Effect of initial MO concentration on initial rate of MO degradation was studied under direct solar light. The initial MO concentration was varied from 5 ppm to 20 ppm, with constant catalyst loading 0.20 g/100 ml. The degradation rate was higher with higher contaminant concentration as shown in Figure (3.15). Turnover number (and quantum yield) values calculated after 40 minutes at different concentrations of MO (5, 10 and 20 ppm) were: 1.972×10^{-3} (0.306×10^{-3}), 3.247×10^{-3} (0.504×10^{-3}) and 0.775×10^{-3} (0.120×10^{-3}) respectively. The increasing on T.N. and Q.Y. values indicate that the rate of photo-degradation increases by increasing the contaminant concentration, to a certain limit. This indicates screening effect by MO particles.

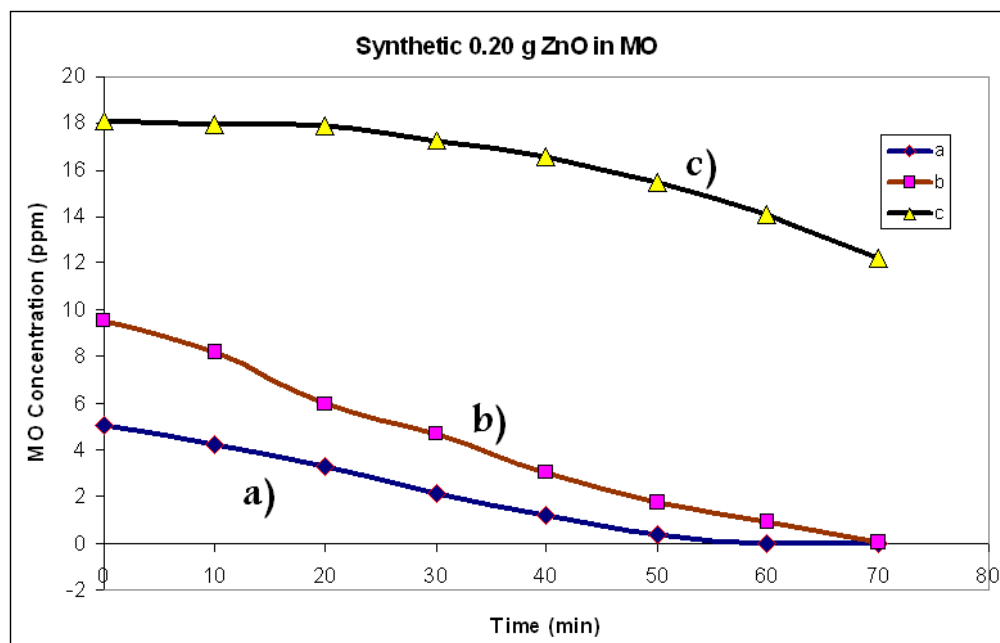


Figure (3.15): Effect of contaminant concentration on photo-degradation reaction using 0.20 g ZnO in 100 mL neutral solution at room temperature under direct solar light (0.0724 W/cm^2). Methyl orange concentrations were: a) 5 ppm b) 10 ppm c) 20 ppm.

3.2.1.4 Effect of Light Concentration

The effect of light concentration was studied using concaved mirrors. The degradation rate was higher with higher light concentration as shown in Figure (3.16). Turnover number (and quantum yield) values calculated after 40 minutes at direct solar light and concentrated solar light were: 2.310×10^{-3} (0.4348×10^{-3}) and 4.252×10^{-3} (0.0889×10^{-3}) respectively. The increasing on T.N. values indicate that the rate of photo-degradation increased by increasing the concentration of solar light, where as Q.Y. values were lowered.

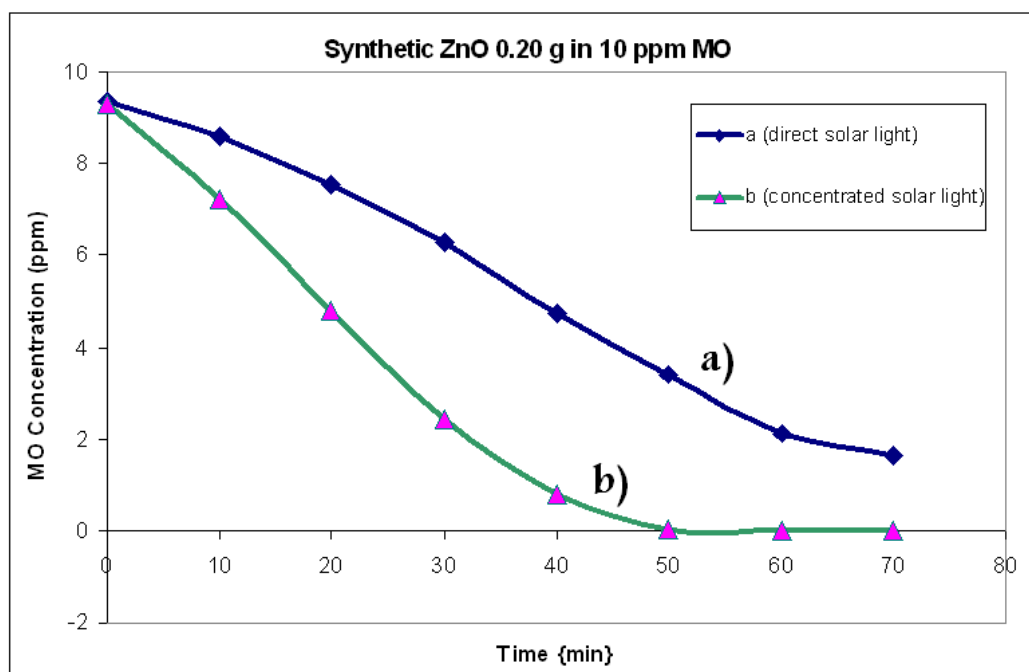


Figure (3.16): Effect of light concentration on photo-degradation of neutral 100 mL solution methyl orange (10 ppm) using 0.20 g ZnO: a) under direct solar light (Radiation Intensity 0.0597 W/cm^2). b) concentrated solar light (Radiation Intensity 0.179 W/cm^2).

3.2.2 Sand-Supported ZnO System (Anneals and Non-Anneals)

3.2.2.1 Effect of pH

Effect of pH on reaction rates of methyl orange degradation with direct solar light and UV-light lamp were investigated. The efficiency of ZnO/Sand system in photo-degradation of methyl orange, with UV-light lamp Figure (3.17) and with solar light Figure (3.18), was investigated at different pH values. Using UV-light lamp Turnover number (and quantum yield) values calculated after 40 minutes at different pH values (7, 9 and 11) were: 2.820×10^{-3} (99.050×10^{-4}), 1.325×10^{-3} (46.540×10^{-4}) and 1.050×10^{-3} (36.880×10^{-4}) respectively. The decreasing on T.N. and Q.Y. values indicate that the rate of photo-degradation decreases by increasing basicity. Using solar light, Turnover number (and quantum yield) values calculated after 40 minutes at pH values (3, 5, 7, 9 and 11) were: 0.220×10^{-3} (3.4354×10^{-4}), 3.245×10^{-3} (5.0673×10^{-4}), 4.055×10^{-3} (6.3321×10^{-4}), 1.775×10^{-3} (2.7718×10^{-4}) and 1.625×10^{-3} (2.538×10^{-3}) respectively. According to previous studies, pH plays an important role in the photo-degradation process of various pollutants [56-62]. For the ZnO/Sand system, the increasing on T.N and Q.Y. values as pH increased from 3 to 7 and become decreased in basic medium (pH > 7) indicate that photo-degradation efficiency increased were at pH 7 the maximum photo-degradation was achieved. In neutral solutions the reaction rates and the turnover number values were higher than in basic or acidic solutions for

both types, The photo-degradation was faster under solar light than under UV lamp light.

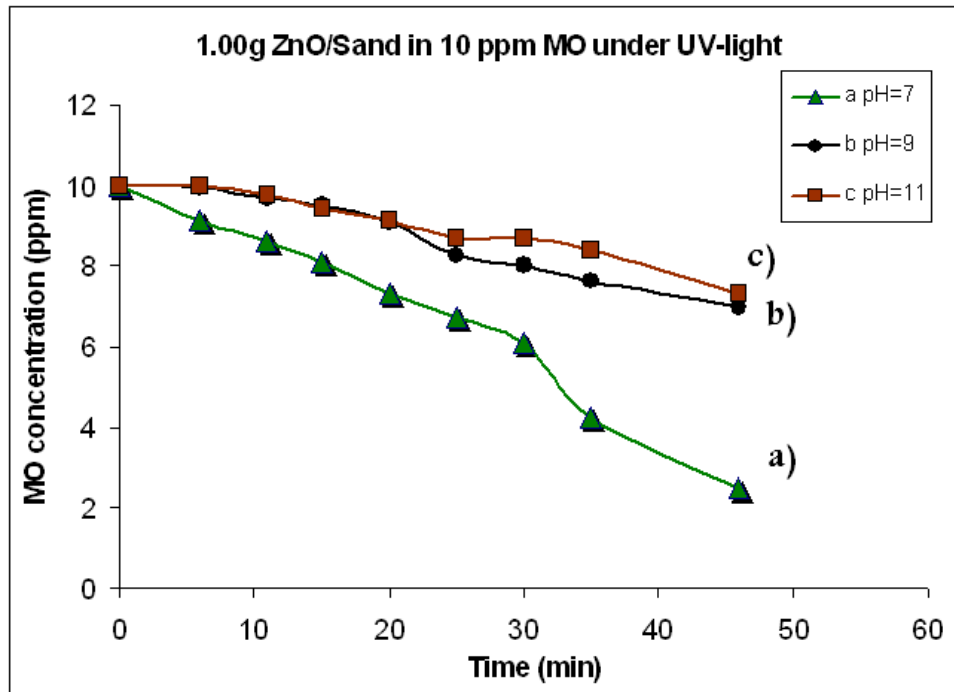


Figure (3.17): Effect of pH on rate of methyl orange degradation reaction. under UV-light (0.0032 W/cm^2). All reactions were conducted at room temperature in a 50 ml solution of methyl orange (10 ppm) using 1.00g ZnO/Sand. The pH values were: a) 7 b) 9 c) 11

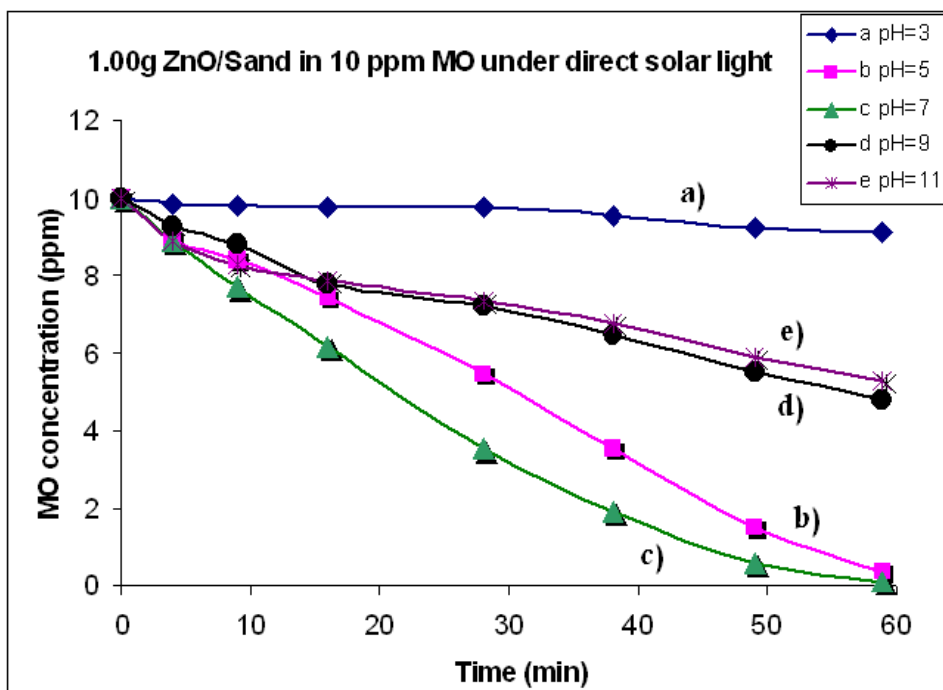


Figure (3.18): Effect of pH on rate of methyl orange degradation reaction. under direct solar light (0.072 W/cm^2). All reactions were conducted at room temperature in a 100 ml solution of methyl orange (10 ppm) using 1.00g ZnO/Sand. The pH values were: a) 3 b) 5 c) 7 d) 9 e) 11

3.2.2.2 Effect of Temperature

The effect of temperature on the rate of MO degradation using ZnO/Sand system was studied within the temperature range $10\text{--}40^\circ\text{C}$. Turnover number (and quantum yield) values calculated after 40 minutes at different temperature values ($10, 20, 30,$ and 40°C), Figure (3.19), were: 0.6950×10^{-3} (1.0369×10^{-4}), 1.010×10^{-3} (1.5069×10^{-4}), 1.235×10^{-3} (1.8426×10^{-4}) and 3.875×10^{-3} (5.7813×10^{-4}) respectively. The increasing on T.N. and Q.Y. values indicate that increasing temperature causes slight increase in the reaction rate. The low calculated value of activating energy ($E_{\text{act}} = 23 \text{ KJ/mol}$) further confirms that. The little enhancement of photodegradation is probably due to the increasing

collision frequency of molecules. Irradiation is believed to be the primary source of e^-/h^+ pairs at ambient temperature because the band gap E_{bg} is too high to overcome by thermal excitation [63] as will be discussed later.

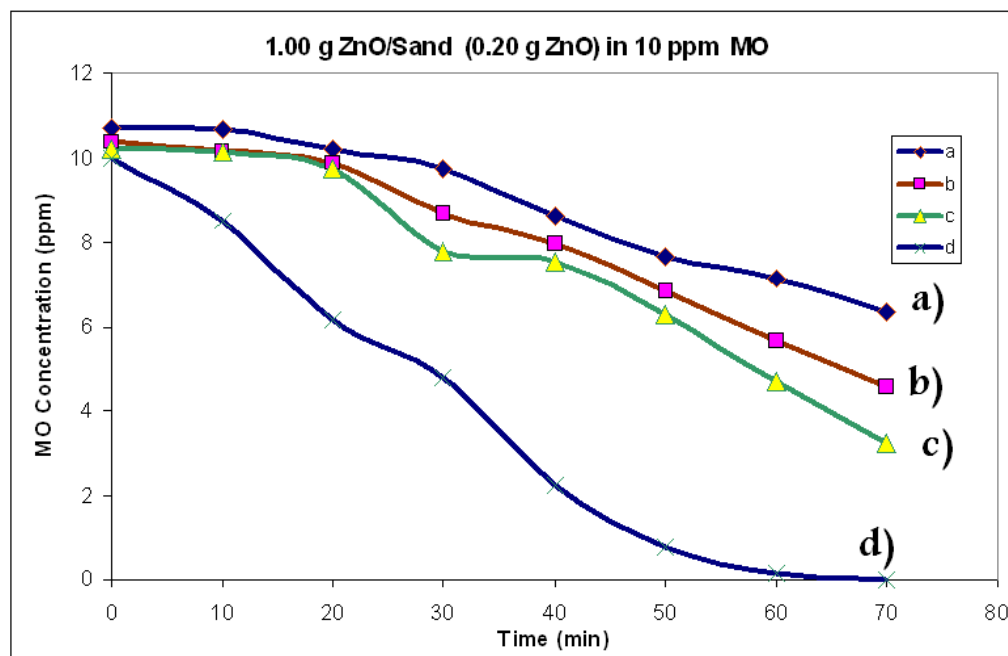


Figure (3.19): Effect of temperature on photo-degradation of neutral 100 mL solution methyl orange (10 ppm) using 1.00 g ZnO/Sand at: a) 10°C b) 20°C c) 30°C d) 40°C. For better temperature control, experiment were conducted in a thermostated reactor using radiation intensity 0.0753 W/cm^2 .

3.2.2.3 Effect of Catalyst Concentration

The effect of concentration of ZnO/Sand on photo-degradation of methyl orange was investigated by varying ZnO/Sand amount from 0.5 to 2 g/100 ml of methyl orange solution with concentration of 10 ppm. Turnover number (and quantum yield) values calculated after 40 minutes for (0.5, 0.75, 1.0, 1.5, and 2.0)g were: 1.30×10^{-3} (0.2236×10^{-3}), 1.38×10^{-3} (0.2374×10^{-3}), 1.75×10^{-3} (0.3002×10^{-3}), 1.45×10^{-3} (0.2495×10^{-3}) and 0.95×10^{-3} (0.1634×10^{-3}) respectively. The increasing on T.N. and

Q.Y. values indicate that the efficiency of reaction increased with increasing catalyst amount to a certain limit. Figure (3.20) shows little change in rate by changing catalyst. In fact rate relatively decreased with higher catalyst nominal concentrations were Sand particles cause shielding of radiations and prevent them from reaching ZnO surface. In case of Sand/ZnO surface, it is assumed that particles on the upper side of reaction mixture only are effectively exposed to UV light. Excessive shielding may lower overall efficiency of the supported catalyst.

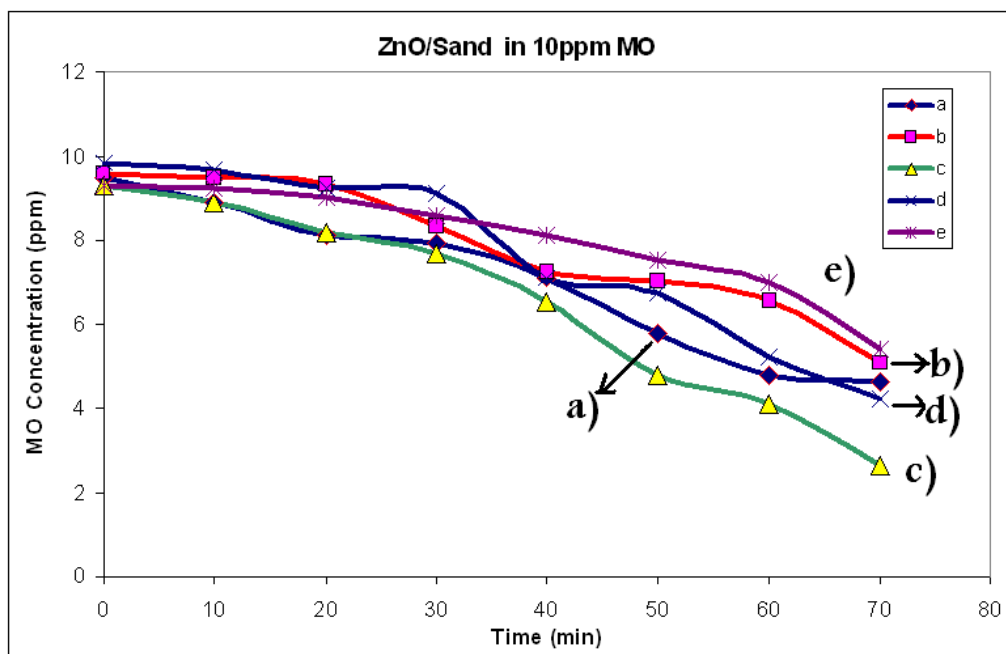


Figure (3.20): Effect of ZnO/Sand catalyst amount on rate of photo-degradation of methyl orange (100 ml solution, 10 ppm), at room temperature under neutral conditions using direct solar light (radiation intensity 0.0653 W/cm^2). Catalyst ZnO/Sand amounts were: a) 0.50g, b) 0.75 g, c) 1.00 g, d) 1.50 g e) 2.00 g.

3.2.2.4 Effect of Contaminant Concentration

Effect of initial MO concentration on initial rate of degradation was studied under direct solar light. The initial MO concentration was varied from 5 ppm to 30 ppm, with constant ZnO/Sand catalyst amount 1.0 g/100 ml. The degradation rate was higher with increasing contaminant concentration, to a certain limit as shown in Figure (3.21). T.N. values (and quantum yield) calculated after 40 minutes for different concentrations of MO (5, 10, 20 and 30 ppm) were: 0.799×10^{-3} (0.122×10^{-3}), 2.99×10^{-3} (0.455×10^{-3}), 1.84×10^{-3} (0.278×10^{-3}) and 0.795×10^{-3} (0.121×10^{-3}) respectively. The increasing on T.N. and Q.Y. values indicate that the rate of photo-degradation increases by increasing the contaminant concentration, to a certain limit. This indicates screening effect by MO particles. The efficiency did not decreased with increasing methyl orange concentration.

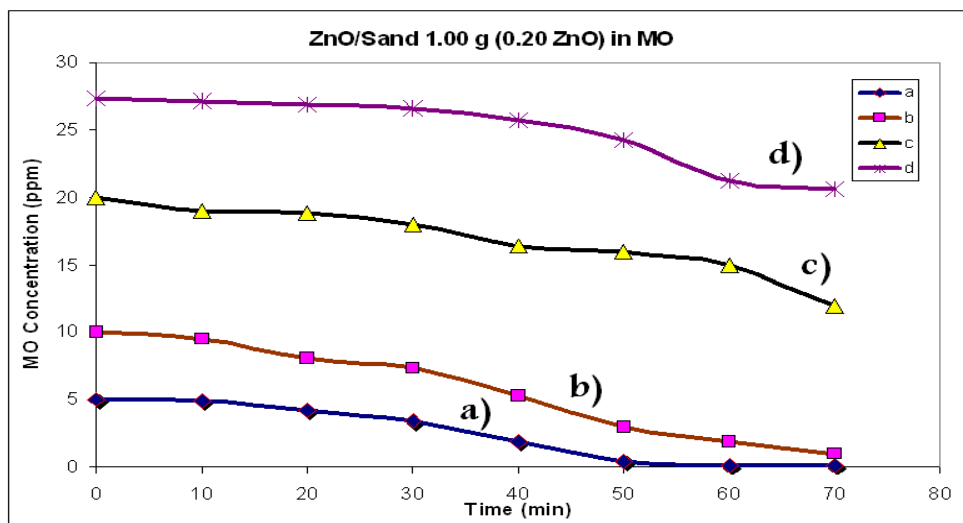


Figure (3.21): Effect of contaminant concentration on photo-degradation reaction using 1.00 g ZnO/Sand in 100 mL neutral solution at room temperature under direct solar light (0.0739 W/cm^2). Methyl orange concentrations were: a) 5 ppm b) 10 ppm c) 20 ppm d) 30 ppm

3.2.2.5 Effect of Light Concentration

The effect of light concentration was studied. The degradation rate was higher with higher light concentration as shown in Figure (3.22). Turnover number (and quantum yield) values calculated after 40 minutes under direct solar light and concentrated solar light were: 2.36×10^{-3} (0.3837×10^{-3}) and 4.502×10^{-3} (0.08132×10^{-3}) respectively. The increasing in T.N. values indicate that the rate of photo-degradation increased by increasing the concentration of solar light, where as Q.Y. values were lowered.

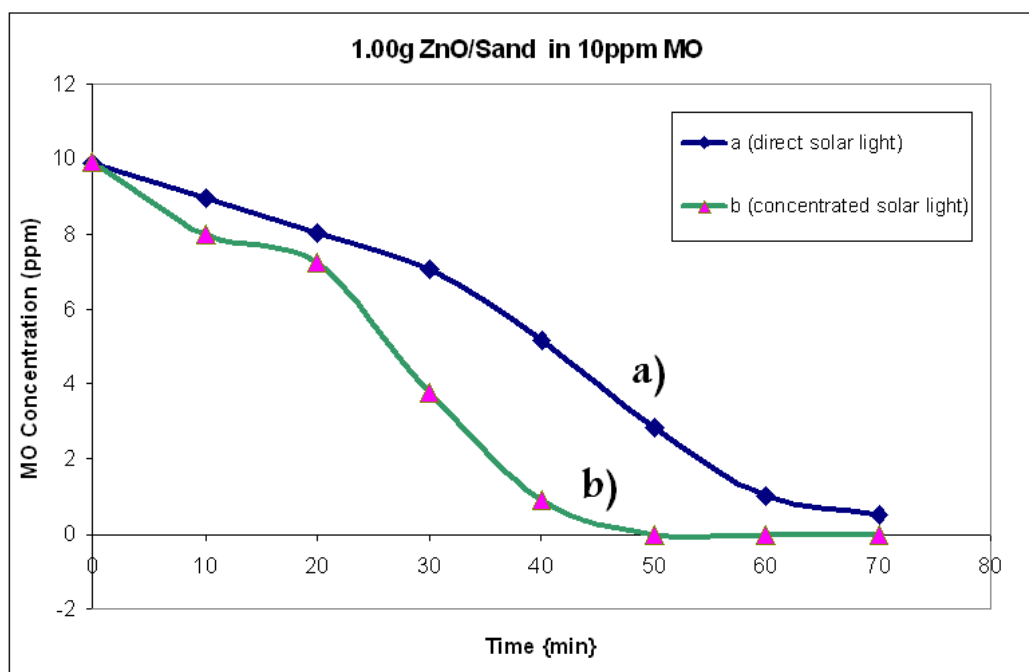


Figure (3.22): Effect of light concentration on photo-degradation of neutral 100 mL solution methyl orange (10 ppm) using 1.00g ZnO/Sand: a) with direct solar light (Radiation Intensity 0.069 W/cm^2). b) Concentrated solar light (Radiation Intensity 0.207 W/cm^2).

3.2.3 Clay-Supported ZnO System (Annealed and Non-Annealed)

1.00g of clay-supported ZnO system (0.200 g ZnO) annealed at different temperatures were compared for photodegradation of 100 ml neutral solution methyl orange with 10 ppm concentration under direct solar light are shown in Figure (3.23). T.N. values were calculated after 40 minutes for ZnO/Clay system with different annealing temperatures (250, and 450 °C). Turnover number (and quantum yield) values are: 2.80×10^{-3} (0.4256×10^{-3}), and 3.26×10^{-3} (0.4955×10^{-3}) respectively. The increasing on T.N. and Q.Y. values indicate that the efficiency of photodegradation increased by increasing the calcination temperature of ZnO/Clay system.

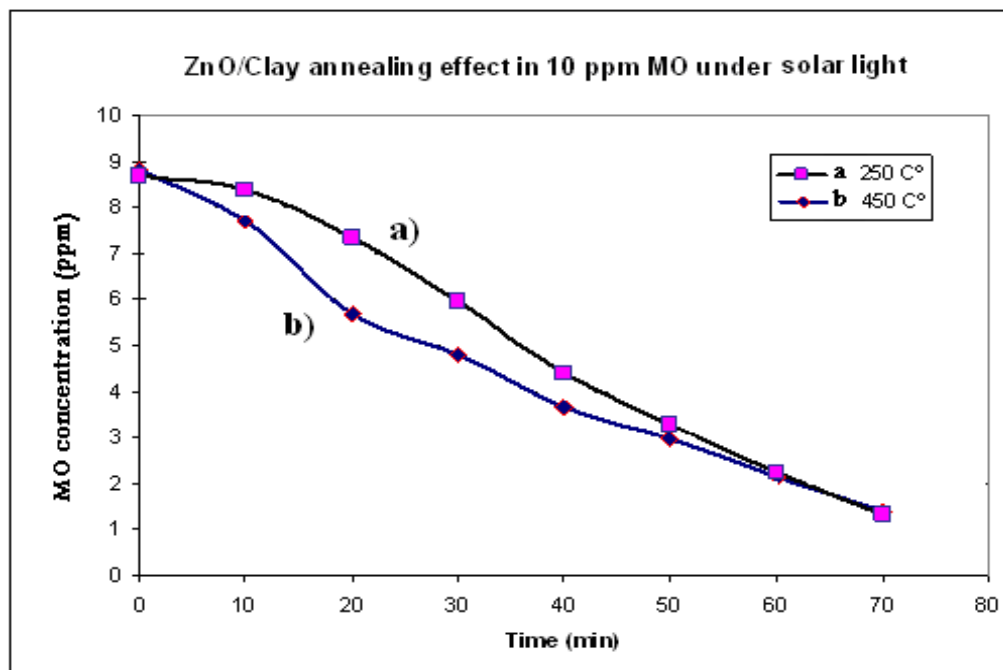


Figure (3.23): Effect of ZnO/Clay annealing on photo-degradation of neutral 100 mL solution methyl orange (10 ppm) using 1.00g ZnO/Clay under direct solar light (Radiation Intensity 0.0737 W/cm^2). : a) 250 °C b) 450 °C.

3.2.3.1 Effect of Temperature

The effect of temperature on the rate of methyl orange degradation using 1.00 g of ZnO/Clay system was studied within the temperature range, 10-40 °C. Turnover number values were calculated after 40 minutes at different temperature values (10, 20, 30, and 40 °C) Figure (3.24). Turnover number (and quantum yield) values were: 1.66×10^{-3} (8.5775×10^{-4}), 2.525×10^{-3} (9.204×10^{-4}), 3.555×10^{-3} (11.3304×10^{-4}) and 3.65×10^{-3} (12.184×10^{-4}) respectively. The increasing on T.N. and Q.Y. values indicate that increasing temperature causes slight increase the reaction efficiency. The low calculated value of activating energy ($E_{act} = 15 \text{ KJ/mol}$) indicate that the rate is only slightly enhanced with increasing the temperature of the reaction as the Figure (3.24) shows.

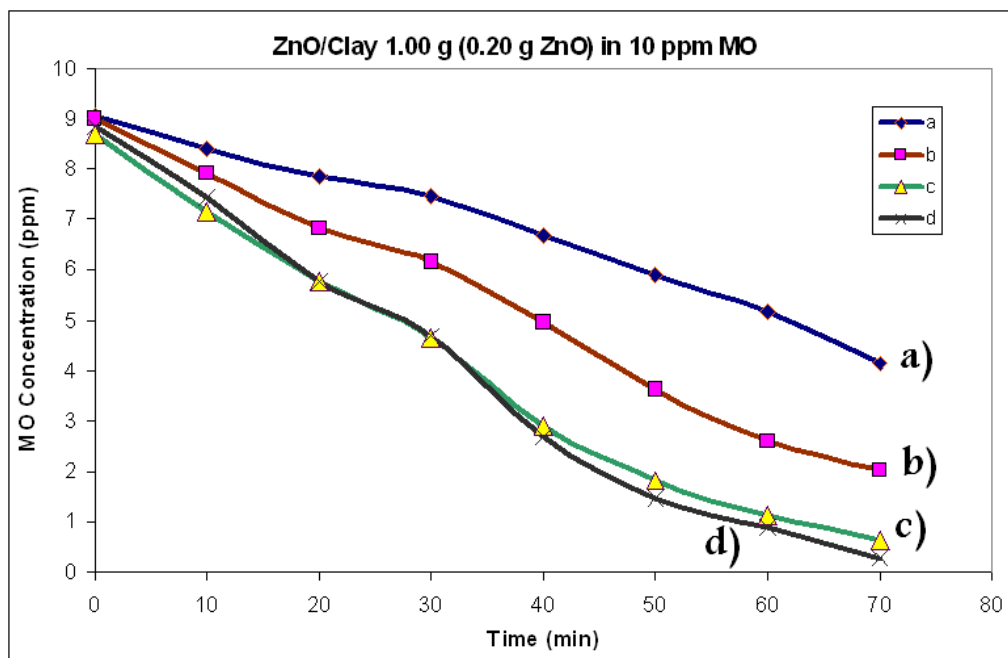


Figure (3.24): Effect of temperature on photo-degradation of neutral 100 mL solution methyl orange (10 ppm) using 1.00 g ZnO/Clay at: a) 10°C b) 20°C c) 30°C d) 40°C. For better

temperature control, radiation was conducted inside thermostated solution of methyl orange under direct solar light (Radiation Intensity 0.0674 W/cm^2)

3.2.3.2 Effect of Catalyst Concentration

The effect of concentration of ZnO/Clay on photo-degradation of methyl orange was investigated by varying ZnO/Clay amount from 0.50 to 2.00 g/100 ml of methyl orange solution with concentration of 10 ppm. The rate of reaction increased with increasing catalyst amount as shown in Figure (3.25). Turnover number (and quantum yield) values calculated after 40 minutes for (0.50, 0.75, 1.00, 1.50, and 2.00)g as ZnO values were: 1.625×10^{-3} (0.30587×10^{-3}), 2.115×10^{-3} (0.3981×10^{-3}), 2.215×10^{-3} (0.4169×10^{-3}), 2.31×10^{-3} (0.4348×10^{-3}) and 2.7×10^{-3} (0.5082×10^{-3}) respectively. The T.N. and Q.Y. values indicate that the rate catalyst efficiency did not decrease as catalyst amount increased.

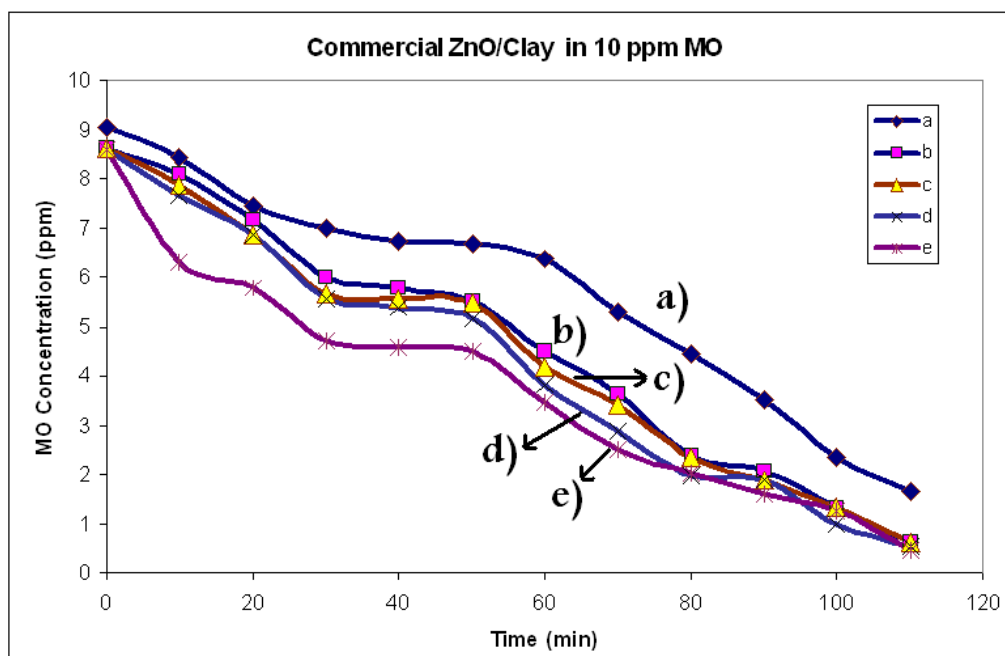


Figure (3.25): Effect of ZnO/Clay catalyst amount on rate of photo-degradation of methyl orange (100 ml solution, 10 ppm), at room temperature under neutral conditions using direct solar light (radiation intensity 0.0597 W/cm^2). ZnO/Clay Catalyst amounts were: a) 0.50g, b) 0.75 g, c) 1.00 g, d) 1.50 g e) 2.00 g.

3.2.3.3 Effect of Contaminant Concentration

Effect of initial MO concentration on initial rate of degradation was studied under direct solar light. The initial MO concentration was varied from 5 ppm to 30 ppm, with constant ZnO/ Clay catalyst amount 1.00 g/100 ml. The degradation rate was higher with contaminant concentration as shown in Figure (3.26). Turnover number (and quantum yield) values calculated after 40 minutes at different concentrations of MO (5, 10, 20 and 30 ppm) were: 1.80×10^{-3} (0.288×10^{-3}), 2.62×10^{-3} (0.419×10^{-3}), 3.60×10^{-3} (0.576×10^{-3}), and 2.16×10^{-3} (0.345×10^{-3}) respectively. The increasing on T.N. and Q.Y. values indicate that the rate of photo-degradation increases by increasing the contaminant concentration, to a certain limit. This indicates screening effect by MO particles. The efficiency did not decreased with increasing methyl orange concentration.

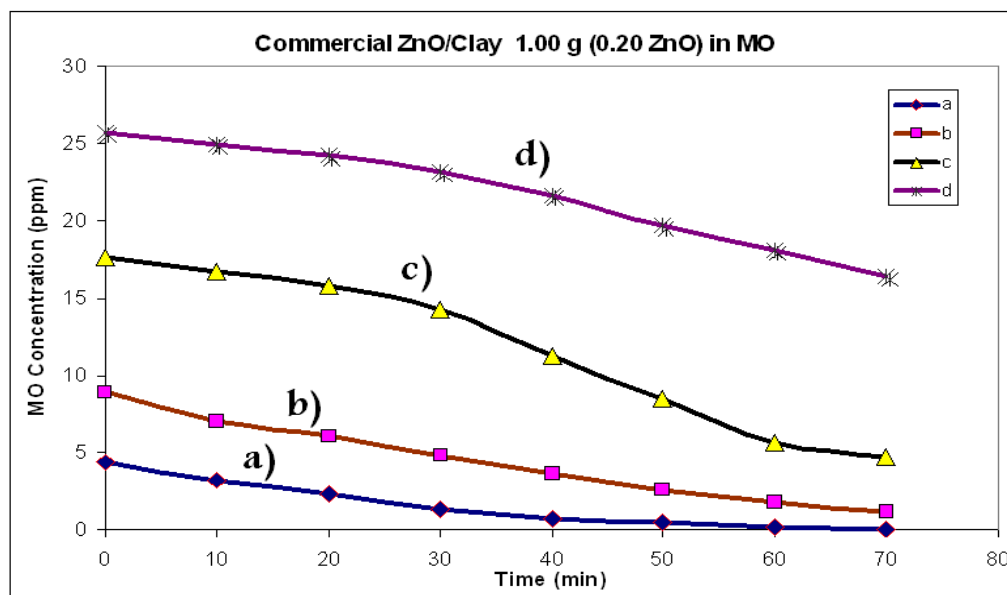


Figure (3.26): Effect of contaminant concentration on photo-degradation reaction using 1.00 g ZnO/Clay in 100 mL neutral solution at room temperature under direct solar light (0.0703 W/cm^2). Methyl orange concentrations were: a) 5 ppm b) 10 ppm c) 20 ppm d) 30 ppm.

3.2.3.4 Effect of Light Concentration

The effect of light concentration on ZnO/Clay catalysed photodegradation was studied. The degradation rate was higher with higher light concentration as shown in Figure (3.27). Turnover number (and Quantum yield) values calculated after 90 minutes under direct solar light and concentrated solar light were: 1.98×10^{-3} (0.2905×10^{-3}) and 3.36×10^{-3} (0.05477×10^{-3}) respectively. The increasing in T.N. values indicate that the efficiency of photo-degradation increased by increasing the concentration of solar light, where as Q.Y. values were lowered.

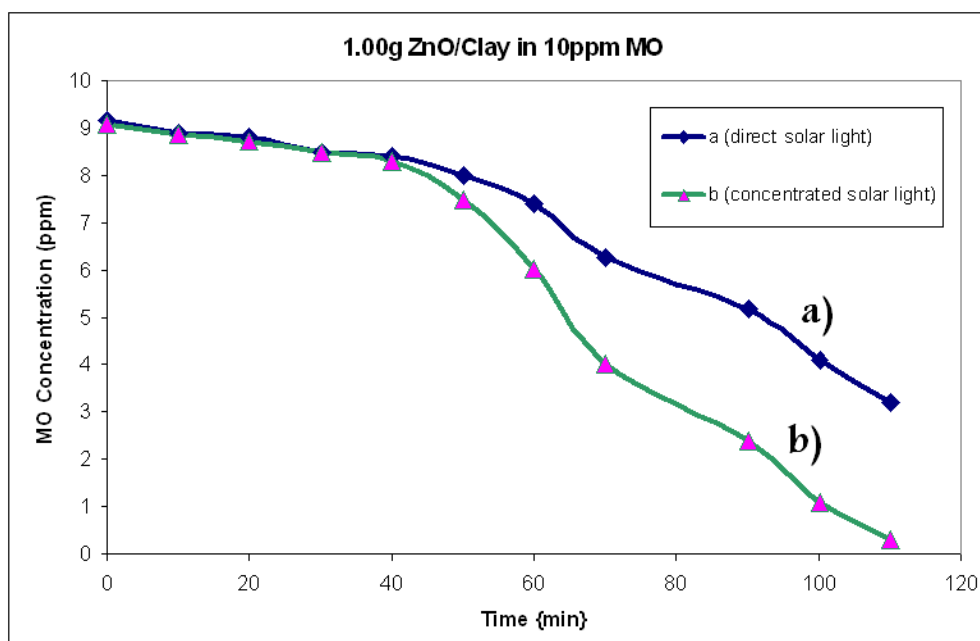


Figure (3.27): Effect of light concentration on photo-degradation of neutral 100 mL solution methyl orange (10 ppm) using 1.00g ZnO/Clay: a) under direct solar light (Radiation Intensity 0.0766 W/cm^2). b) Concentrated solar light (Radiation Intensity 0.2297 W/cm^2).

3.2.4 AC-Supported ZnO System (Annealed and Non-Annealed)

Control experiments were conducted using aqueous methyl orange solutions, in the absence of light and in the absence of catalyst. Control experiments were also conducted using aqueous methyl orange solutions in the absence of catalyst while using activated carbon (AC). It was found that in all photolysis experiments, carried out with no catalyst, or no light, no methyl orange concentration loss occurred after prolonged time when naked ZnO was used. ZnO/AC system exhibited adsorption of methyl orange onto the AC surface, which accounted for about 17 ppm of contaminant concentration on the AC surface (0.02 g). This adsorption was considered while conducting photodegradation experiments.

3.2.4.1 Effect of Temperature

Methyl orange (50 ppm) degradation was studied using 0.120 g of AC/ZnO system at different temperatures, as shown in Figure (3.28). Turnover number (and quantum yield) values calculated after 40 minutes at different temperature values (10, 20, 30, and 40 °C) were: 1.66×10^{-3} (8.5775×10^{-4}), 2.525×10^{-3} (9.204×10^{-4}), 3.555×10^{-3} (11.3304×10^{-4}) and 3.65×10^{-3} (12.184×10^{-4}) respectively. The increasing on T.N. and Q.Y. values indicate that increasing temperature causes slight increase in the reaction efficiency. The low calculated value of activating energy ($E_{act} = 8$ KJ/mol) indicate that the rate is only slightly enhanced with increasing the temperature of the reaction as the Figure (3.28) shows.

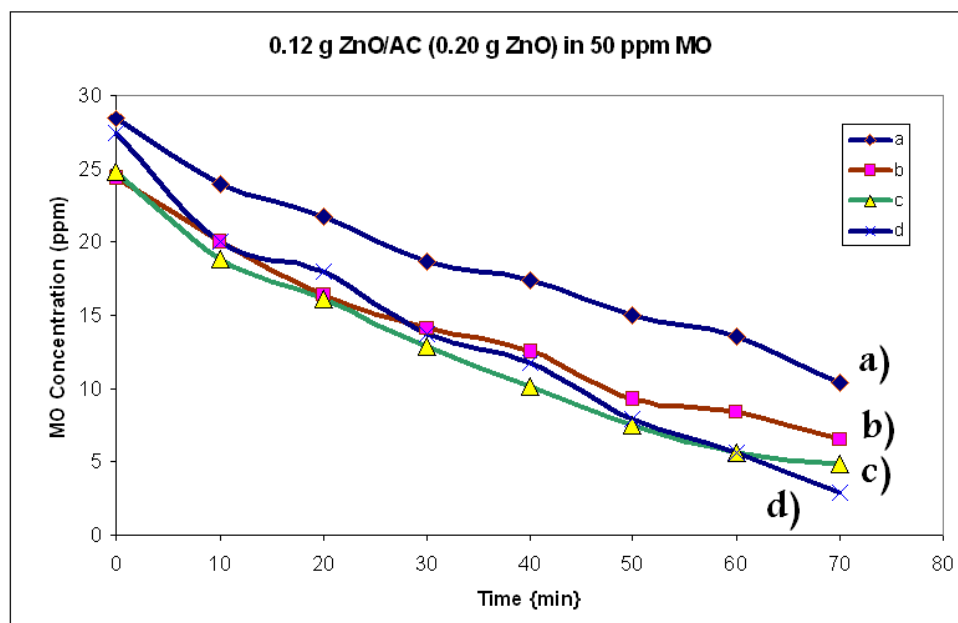


Figure (3.28): Effect of temperature on photo-degradation of neutral 100 mL solution methyl orange (50 ppm) using 0.120 g ZnO/AC at: a) 10°C b) 20°C c) 30°C d) 40°C. For better temperature control, radiation was conducted inside thermostated solution of methyl orange under direct solar light (Radiation Intensity 0.0724 W/cm²)

3.2.4.2 Effect of Catalyst Concentration

The methyl orange degradation reaction was studied using different ZnO/AC nominal amounts from 0.072 to 0.144 g/100 ml methyl orange solution with concentration of 50 ppm. Turnover number (and quantum yield) values calculated after 40 minutes for 0.072, 0.096, 0.120 and 0.144g were: 0.650×10^{-3} (0.1090×10^{-3}), 3.25×10^{-3} (0.5451×10^{-3}), 8.50×10^{-3} (1.426×10^{-3}) and 7.50×10^{-3} (1.259×10^{-3}) respectively. The T.N. and Q.Y. values indicate that the efficiency of reaction increased with increasing catalyst amount. Were the rate increased as shown in Figure (3.29). At higher catalyst nominal concentrations the rate decreased.

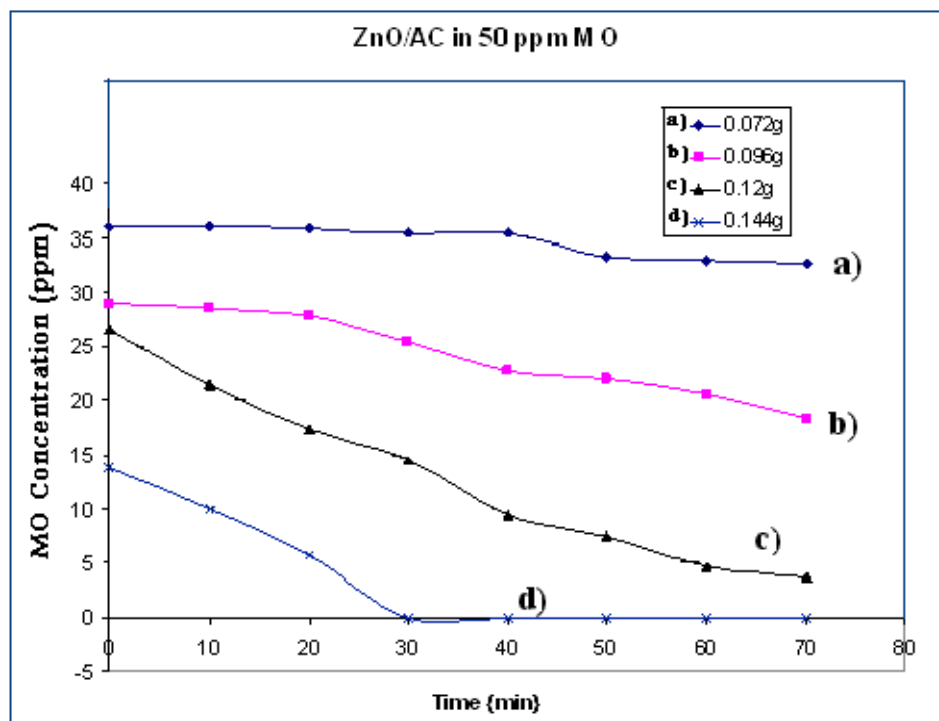


Figure (3.29): Effect of ZnO/AC catalyst amount on rate of photo-degradation of methyl orange (100 ml solution, 50 ppm), at room temperature under neutral conditions using direct solar light (radiation intensity 0.067 W/cm^2). ZnO/AC Catalyst amounts were: a) 0.072g, b) 0.096 g, c) 0.120 g, d) 0.144 g

3.2.4.3 Effect of Contaminant Concentration

Effect of initial methyl orange concentration on initial rate of degradation was studied under direct solar light. The initial MO concentration was varied from 20 ppm to 50 ppm, with constant ZnO/AC catalyst amount 0.120 g/100 ml. The degradation rate was higher with contaminant concentration as shown in Figure (3.30).

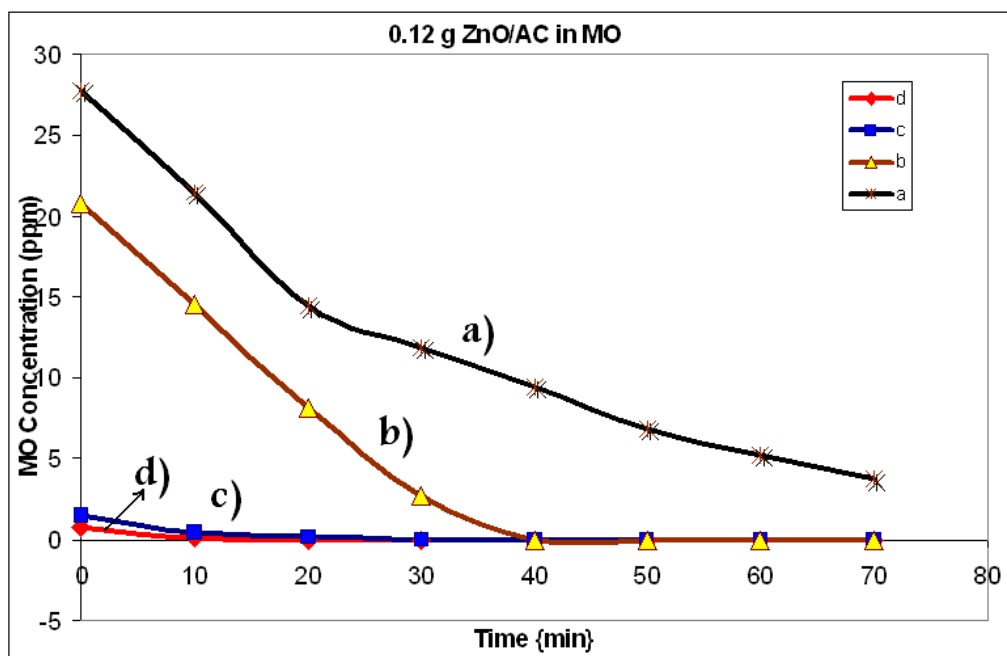


Figure (3.30): Effect of contaminant concentration on photo-degradation reaction using 0.120g ZnO/AC in 100 mL neutral solution at room temperature under direct solar light (0.0634 W/cm^2). Methyl orange concentrations were: a) 20 ppm b) 30 ppm c) 40 ppm d) 50 ppm.

3.2.4.4 Effect of Light Concentration

The effect of light concentration was studied for ZnO/AC catalysed photodegradation. The degradation rate was slightly higher with higher light concentration as shown in Figure (3.31). Turnover number values (and quantum yield) values calculated after 90 minutes under direct solar light and concentrated solar light were: 14.29×10^{-3} (2.394×10^{-3}) and 17.80×10^{-3} (0.995×10^{-3}) respectively. The increasing in T.N. values indicate that the efficiency of photo-degradation increased by increasing the concentration of solar light, where as Q.Y. values were lowered.

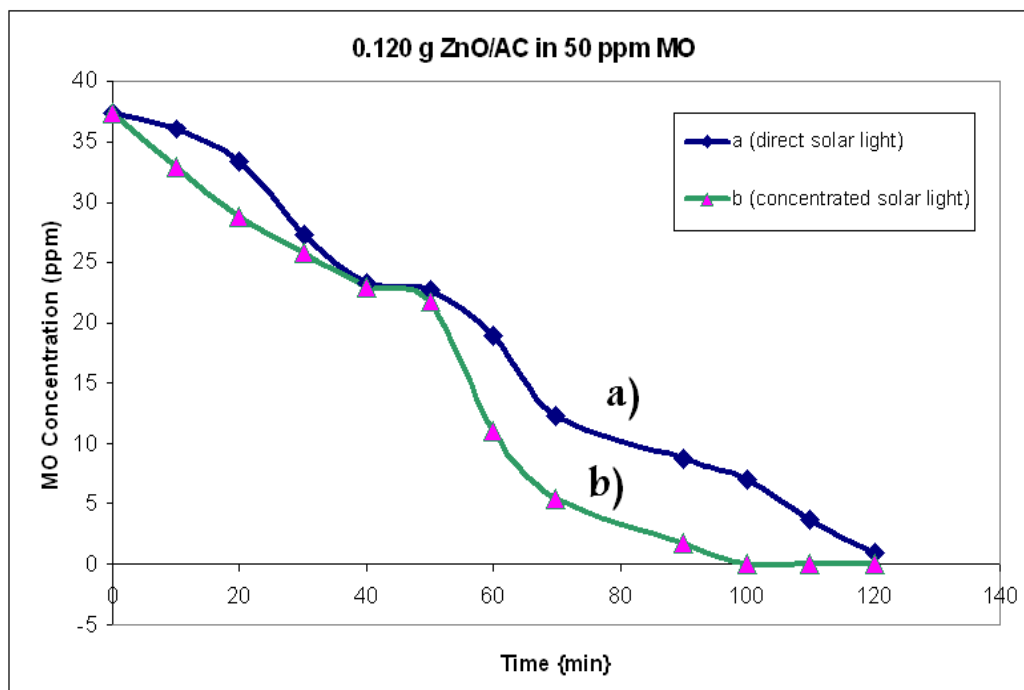


Figure (3.31): Effect of light concentration on photo-degradation of neutral 100 mL solution methyl orange (50 ppm) using 0.120g ZnO/AC: a) direct solar light (Radiation Intensity 0.067 W/cm²). b) Concentrated solar light (Radiation Intensity 0.201 W/cm²).

3.2.5 Thin Film ZnO System

3.2.5.1 Effect of Light Concentration

The effect of light concentration was studied for thin film ZnO system catalysed photodegradation was studied. The degradation rate was higher with higher light concentration as shown in Figure (3.32).

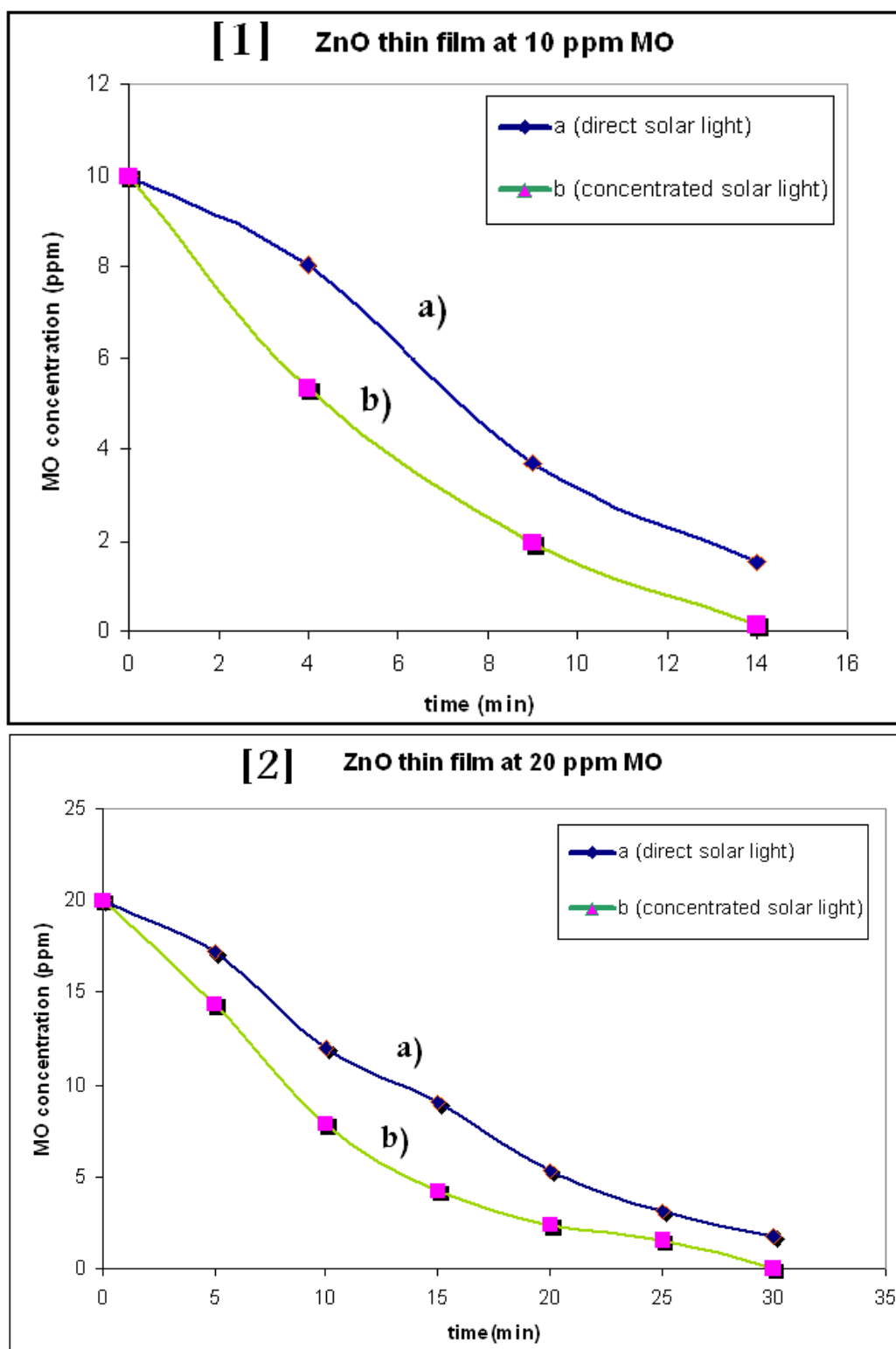


Figure (3.32): Effect of light concentration on photo-degradation of neutral 100 mL solution methyl orange ([1] 10 ppm, [2] 20 ppm) using ZnO thin film: a) direct solar light (Radiation Intensity 0.067 W/cm^2). b) Concentrated solar light (Radiation Intensity 0.201 W/cm^2).

CHAPTER 4

DISCUSSIONS

4.1 General

Both commercial (microscale) and synthetic (nanoscale) ZnO particles catalyzed photodegradation of methyl orange (MO) in aqueous media. Different parameters were investigated in this study. Effect of nature of light was studied. Effect of pH was studied, and the neutral medium showed better activity, thus pH 7 was used unless otherwise stated. Type of ZnO particles showed little effect. Supporting ZnO onto AC increased the rate of the reaction. Results presented in chapter 3 are discussed here.

4.2 Photoluminescence for ZnO Systems:

The photoluminescence Emission spectra for synthetic ZnO systems, are shown in Table (4) below.

Table (4) Photoluminescence emission spectral wavelength values for ZnO systems.

ZnO system	Synthetic non-annealed	Sonicated synthetic non-annealed	Commercial non-annealed	Synthetic Annealed at 600 °C
Wavelength Spectra (nm)	395	390	400	397

It is observed that the commercial ZnO has the longest emission wavelength due to its larger particle size. The sonication decreased the particle size compared to non-sonicated one, so the wave length became shorter. Finally it is observed that the annealed system had longer wave length because annealing increased the particle size by sintering. This is consistent with earlier literature [64-66].

4.3 X-ray Diffraction (XRD) :

Table (5) : Particle size values for different synthetic ZnO systems .

1) Synthetic ZnO	Average particle diameters D (nm)
a) Non-annealed sonicated	21.8
b) Non-annealed non-sonicated	21.8
c) Annealed non-sonicated	24
2) ZnO/sand system Commercial ZnO supported onto sand.	
a) Annealed at 250 °C	19.7
b) Annealed at 450 °C	25
3) ZnO/Clay system Commercial ZnO supported onto clay.	
a) Annealed at 250 °C	24
b) Annealed at 450 °C	25.2
4) ZnO/AC system Synthetic ZnO supported onto activating carbon	
a) Non-annealed	20.8
b) Annealed at 200 °C	23

XRD spectra for all systems resemble each other, as explained in sections (3.1.1.3), (3.1.2.1), (3.1.3.1) and (3.1.4.1) with only small shifting. The dominant crystal structure was hcp. From the XRD analyses and the Scherrer equation, we observed that annealing increased particle diameter

D as summarized in Table (5). The particle size become larger for annealed systems compared to their non-annealed counterparts.

We used commercial ZnO (230 nm) to be attached to sand and clay particles. During mixing in aqueous solution, the ZnO became in equilibrium with ZnO(OH)₂. In the vaporization process the ZnO(OH)₂ reformed ZnO nano-particles to have smaller size in range (20-25 nm). This result is confirmed by XRD patterns as summarized in Table (5).

4.4 SEM Results:

SEM images were recorded for ZnO/AC (synthetic) system only. The images indicate that ZnO particles were flake-shaped particles with uniform thickness of 21 nm thickness. This value confirms that obtained from XRD results in section (3.1.4.1) showing average diameter of about 21 nm.

4.5 Photocatalytic Degradation of MO:

Figures (3.11) and (3.12) showed that the reaction rate under direct solar light was greater than under UV-lamp light. This was due to the concentration of photons that reach the surface of catalyst. This is due to low working power of the lamp giving only line spectra at certain wavelengths as shown in Fig.(2.2). Annealing slightly enhanced the catalyst efficiency. The time of stirring during catalyst preparation also

affected rate of photocatalysis reaction. This is consistent with earlier studies [67].

4.5.1 pH Effect.

According to earlier studies, pH plays an important role in the photo-degradation process of various pollutants [56-62]. For the ZnO/Sand system a high increase in photo-degradation was observed as pH increased from 3 to 7, and then decreased above pH 7. At pH 7 the maximum photo-degradation efficiency was achieved. The low initial reaction rates under acidic or basic conditions are due to dissolution and photodissolution of ZnO see Fig (3.20) [68]. The ZnO exhibits amphoteric behavior. At acidic pH, ZnO can react with acids to produce the corresponding salt, where at alkaline pH, it reacts with a base to form complexes like $[\text{Zn}(\text{OH})_4]^{2-}$. So in neutral solutions the reaction rates and the turnover number values were higher than in basic or acidic solutions for both types.

4.5.2 Effect of Photoreaction Temperature.

Using the Arrhenius equation, values of activation energy were measured. Low values of activation energy were found for synthetic ZnO nano-particle powder, for ZnO/Clay and ZnO/AC systems. The values were only 8.90, 14.7 and 7.90 KJ/mole respectively.

Unlike thermal catalytic reactions, photo-degradation reactions are known to be insensitive to temperature [69]. Photochemical degradation

reactions, using high band gap semiconductor (SC) catalysts, normally have rates that are known to be independent of temperature [70-71]. Energy provided by heating is relatively small; heating to 40°C (313 K) provides only a fraction of an electron volt, which is far less than needed to excite the high-band gap ZnO. Moreover, at higher temperatures, contaminant molecules may become more desorbed away from catalyst surface, which lowers the reaction rate [72]. Higher temperatures are also responsible for removal of oxygen from the reaction mixture which is necessary for contaminant oxidation [73].

The highest activation energy observed was for ZnO/Sand system with 23 KJ/mol value. The little enhancement of photodegradation is probably due to increasing collision frequency of molecules. Irradiation is believed to be the primary source of e^-/h^+ pairs at ambient temperature because the band gap E_{bg} is too high to overcome by thermal excitation [63].

4.5.3 Effect of Catalytic Concentration.

For synthetic ZnO nano-particle powder the T.N. and Q.Y. values show that the efficiency increased with increasing ZnO amount. At higher concentrations the rate decreased. This is due to screening effect by ZnO particles causing reduction in light penetration inside solution and a consequent rate decrease [74]. For ZnO/Sand and ZnO/AC systems the rate decreased with higher catalyst nominal concentrations. This is because

sand and activated carbon particles cause shielding of radiations and prevent them from reaching ZnO surface. In case of ZnO/Sand surface, it is assumed that only particles on the upper side of reaction mixture are effectively exposed to suitable UV light. This should lower overall efficiency of the supported catalyst as shown in Figures (3.20) and (3.29). For ZnO/Clay system the rate of reaction increased with increasing of catalytic amount as shown earlier in Figure (3.25).

4.5.4 Effect of Contaminant Concentration.

For synthetic ZnO nano-particle powder the T.N. values show that the rate of photo-degradation increases by increasing the contaminant concentration, to a certain limit. This indicates screening effect by MO particles. For ZnO/Sand and ZnO/Clay systems the rate of photo-degradation increases by increasing the contaminant concentration, to a certain limit. This indicates screening effect by MO particles as shown in Figures (3.21) and (3.26). This is consistent with earlier studies [75-78].

4.5.5 Effect of Light Concentration.

From T.N. values, Figures (3.16), (3.22), (3.27) and (3.31), indicate that the rate of photo-degradation increased by increasing the concentration of solar light for all studied ZnO systems. This is consistent with earlier studies [31, 79-80]. It should be noted that the Q.Y. values slightly decreased, which is possibly due to loss of incident photons where the

overall quanta of light absorbed by any photocatalyst or reactant is given by:

$$Q.Y = (\text{number of reacted molecules})/(\text{number of incident photons})$$

Where the number of reacted molecules accounts for moles of methyl orange (MO) consumed and the number of incident photons relates to the amount of photons at wavelength λ absorbed by ZnO systems.

The light scattering in solid–liquid regimes is particularly significant. Q.Y. is thus experimentally difficult to determine as metal oxides in a heterogeneous regime including catalyst cannot absorb all the incident radiation due to refraction [81]. Another factor which limits photonic efficiency (ζ_r) is the thermal recombination between electrons and holes [82]. For these reasons, it is argued that references to Q.Y. or efficiency in heterogeneous system are not advised despite previous use of the term by previous references [83-84].

4.6 Effect of Annealing

Annealing at (250 and 450) °C for ZnO/Clay and ZnO/Sand systems, at 200 °C for ZnO/AC, and at 600 °C for synthetic zinc oxide, under air pressure was conducted from T.N. values, Figures (3.11), (3.12), and (3.23), indicate that the annealing increased efficiency for all ZnO systems. This is because the energy gap of ZnO decreases with increasing annealing temperature, and threshold absorption wavelength increases, since size of

the ZnO particle increase with increasing annealing temperature. It can thus be concluded that photocatalytic activity of ZnO is enhanced with higher annealing temperature. The enhanced photocatalytic activity of ZnO might be ascribed to the increase of grain size and the oxygen defect density. This is consistent with earlier studies [64].

With increasing of annealing temperature, the average size of ZnO nanoparticles increased. The bonding structure of acetate groups coordinating with zinc ions evolved from unidentate to bidentate type, cause photocatalytic stability in the whole catalytic process for the stable bidentate bonding type of acetate groups [61]. From earlier studies particle size of ZnO powder were found to increase with increasing the enthalpy density, and high-temperature residence time during preparation and improved crystalline quality of ZnO nanoparticles [66].

CONCLUSIONS:

- 1- Different types of naked and supported nano ZnO particles were prepared and characterized. All systems showed catalytic activity in methyl orange photodegradation.
- 2- Supporting the ZnO onto activated carbon enhanced the photodegradation reaction rates.
- 3- Solar light showed higher efficiency than UV-light lamp.
- 4- Under neutral conditions (pH=7) the photodegradation process was faster than either acidic or basic conditions.
- 5- Annealing the catalyst enhanced the reaction rates for all photodegradation systems.
- 6- Contaminant molecule adsorb onto activated carbon and clay but not on sand supports.
- 7- Methyl orange photodegradation rate increased with increasing solar light concentration, but quantum yield values decreased.

SUGGESTIONS FOR FURTHER WORK:

- 1- Degrade other water contaminants, such as drug formulations, fertilizers, chlorinated hydrocarbons, insecticides, pesticides, phenols and others using ZnO/AC, ZnO/Sand, and ZnO/Clay systems.
- 2- Use photodegradation process of ZnO systems in purification of soil and air.
- 3- Use thin films of ZnO on glass, plastic and ceramic in photodegradation of water contaminants.
- 4- Applying thin film ZnO system in photodegradation more water organic contaminants.

References

1. A. Fujishima and K. Honda. **"Electrochemical photolysis of water at a semiconductor electrode"**. *Nature* **238.5358** (1972); 37-38.
2. M. R. Hoffman, S. T. Martin, W. Choi, D. W. Bahnemann, **"Environmental Applications of Semiconductor Photocatalysis"**. *Chem. Rev.* **95** (1995); 69-96.
3. J. Peral, X. Domenech, D. F. Ollis, **"Heterogeneous photocatalysis for purification, decontamination and deodorization of air"**. *J. Chem. Tech. Biotech.*, **70** (1997); 117.
4. X. Chen: Doctoral Dissertation, **"Synthesis and Investigation of Novel Nanomaterials for Improved Photocatalysis"**. *Case Western Reserve University*, August (2005).
5. C. S. Turchi, and D. F. Ollis, **"Photocatalytic degradation of organic water contaminants: Mechanisms involving hydroxyl radical attack"**. *J. Cat.*, **122** (1990); 178.
6. D. Lev: Doctoral Dissertation, **"Photocatalytic Degradation of Organic Contaminants: Novel Catalysts and Processes"**. *Mendeleev Institute*, June (2001).
7. Y. Ohko, T. Tatsuma, A. Fujishima, **"Characterization of TiO₂ Photocatalysis in the Gas Phase as a Photoelectrochemical System: Behavior of Salt-Modified System"**. *J. Phys. Chem.*, **105** (2001)10016.
8. M. R. Dhananjeyan, J. Kiwi, and K. R. Thampi, **"Fe₂O₃ immobilized on derivatized polymer films for mineralization of pollutants"**. *Chem. Commun.* (2000) 1443.
9. M. R. Dhananjeyan, E. Mielczarski, K. R. Thampi, Ph. Buffat, M. Bensimon, A. Kulik, J. Mielczarski, J. Kiwi, **"Photodynamics and Surface Characterization of TiO₂ and Fe₂O₃ Photocatalysts Immobilized on Modified Polyethylene Films"**. *J. Phys. Chem. B* **105** (2001); 12046.
10. F. Zhang, J. Zhao, H. Hidaka, E. Pelizetti, N. Serpone, **"TiO₂-assisted photodegradation of dye pollutants II. Adsorption and**

degradation kinetics of eosin in TiO₂ dispersions under visible light irradiation". *Appl. Catal. B: Environ.* **15 (1998); 147.**

11. G. Al-Sayyed, J. C. D'Oliveira, P. Pichat, "**Semiconductor-Sensitized Photodegradation of 4-Chlorophenol in water**". *J. Photochem. Photobiol. A: Chem.* **58** (1991); 99.

12. D. F. Ollis, H. Al-Ekabi, "**Photocatalytic Purification of Water and air**". Elsevier, Amsterdam, The Netherlands, 1993.

13. K. R. Thampi, J. Kiwi and M. Graetzel, "**Methanation and photo-methanation of carbon dioxide at room temperature and atmospheric pressure**". *Nature* **327** (1987); 506.

14. K. R. Thampi, P. Ruterana and M. Graetzel, "**Low-Temperature Thermal and Photoactivation of TiO₂-Supported Ru, Rh, and Cu Catalysts for CO-NO Reaction**". *J. Catal.* **126** (1990); 572.

15. J. C. Colmenares, R. Luque, J. M. Campelo, F. Colmenares, Z. Karpiński, A. A. Romero, "**Nanostructured Photocatalysts and Their Applications in the Photocatalytic Transformation of Lignocellulosic Biomass: An Overview**". *Materials.* **2** (2009); 2228-2258.

16. M. C. Markham, M. C. Upreti, "**Photoelectric effects at semiconductor electrodes**". *J. Catal.* **4** (1965) 229.

17. P. V. Kamat, "**Photochemistry on nonreactive and reactive (semiconductor) surfaces**". *Chem. Rev.* **93** (1993) 267.

18. S. Sakthivel, B. Neppolian, M. V. Shankar, B. Arabindoo, M. Palanichamy, V. Murugesan, "**Solar photocatalytic degradation of azo dye: comparison of photocatalytic efficiency of ZnO and TiO₂**". *Sol. Energy Mater. Sol. Cells.* **77** (2003); 65–82.

19. C. A. K. Gouvea, F. Wypych, S. G. Moraes, N. Duran, N. Nagata, P. Peralta-Zamora, "**Semiconductor-assisted photocatalytic degradation of reactive dyes in aqueous solution**". *Chemosphere* **40** (2000); 433–440.

20. C. Lizama, J. Freer, J. Baeza, H. D. Mansilla, "**Optimized Photodegradation of Reactive Blue 19 on TiO₂ and ZnO suspensions**". *Catal. Today* **76** (2002); 235–246.

21. P. V. Kamat, R. Huehn, R. Nicolaescu, **"A 'sense and shoot' approach for photocatalytic degradation of organic contaminants in water"**. *J. Phys. Chem. B* **106** (2002); 788–794.
22. R. Comparelli, E. Fanizza, M. L. Curri, P. D. Cozzoli, G. Mascolo, A. Agostiano, **"UV-induced photocatalytic degradation of azo dyes by organic capped ZnO nanocrystals immobilized onto substrates"**. *Appl. Catal. B: Environ.* **62** (2005); 144–149.
23. O. A. Fouad, A. A. Ismail, Z. I. Zaki, R. M. Mohamed, **"Zinc oxide thin films prepared by thermal evaporation deposition and its photocatalytic activity"**. *Appl. Catal. B: Environ.* **62** (2006) 144–149.
24. M. C. Yeber, J. Roderiguez, J. Freer, J. Baeza, N. Duran, H. D. Mansilla, **"Advanced oxidation of a pulp mill bleaching wastewater"**. *Chemosphere* **39** (1999) 1679-1688.
25. A. A. Khodja, T. Sheili, J. F. Pihichowski, P. Boule, **"Photocatalytic degradation of 2-phenylphenol on TiO₂ and ZnO in aqueous suspensions"**. *J. Photochem. Photobiol. A: Chem.* **141** (2001); 231–239.
26. N. Serpone, P. Maruthamuthu, P. Pichat, E. Pelizzetti, H. Hidaka, **" Exploiting the interparticle electron-transfer process in the photocatalyzed oxidation of phenol, 2-chlorophenol and pentachlorophenol—chemical evidence for electron and hole transfer between coupled semiconductors, "** *J. Photochem. Photobiol. A: Chem.* **85** (2001); 247–253.
27. S. Sakthivel, B. Neppolian, M. V. Shankar, B. Arabindoo, M. Palanichamy, V. Murugesan, **"Solar photocatalytic degradation of azo dye: comparison of photocatalytic efficiency of ZnO and TiO₂"**. *Sol. Energy Mater. Sol. Cells* **77** (2003); 65–82.
28. A. Sharma, P. Rao, R. P. Mathur, S. C. Ameta, **"Photocatalytic reactions of xylidine ponceau on semiconducting zinc oxide powder"**. *J. Photochem. Photobiol. A: Chem.* **86** (1995); 197–200.
29. I. Poullos, I. Tsachpinis, **"Photodegradation of the textile dye Reactive Black 5 in the presence of semiconducting oxides"**. *J. Chem. Technol. Biotechnol.* **74** (1999); 349–357.

30. C. A. K. Gouvêa, F. Wypych, S. G. Moraes, N. Duran, N. Nagata, P. Peralta-Zamora, "**Semiconductor-assisted photocatalytic degradation of reactive dyes in aqueous solution**". *Chemosphere* **40** (2000); 433.
31. S. Dindar, J. Icli, "**Unusual photoreactivity of zinc oxide irradiated by concentrated sunlight**". *J. Photochem. Photobiol. A: Chem.* **140** (2001); 263.
32. N. Daneshvar, S. Aber, M. S. Seyed Dorraji, A. R. Khataee, and M. H. Rasoulifard, "**Preparation and Investigation of Photocatalytic Properties of ZnO Nanocrystals: Effect of Operational Parameters and Kinetic Study**". *Int. J. Chem. Biomol. Eng.* **1** (2008); 24-29.
33. C. P. Poole Jr, and F. J. Owens, "**Introduction to nanotechnology**" John Wiley & Sons Inc., Hoboken, New Jersey (2003).
34. G. Yuan and M. A. Keane, "**Liquid phase catalytic hydrodechlorination of 2,4 dichlorophenol over carbon supported palladium: an evaluation of transport limitations**". *Chem. Eng. Sci.*, **58** (2003); 257-267.
35. A. H. Zyoud and H. S. Hilal, Silica-Supported CdS-Sensitized TiO₂ Particles in Photo-Driven Water Purification: Assessment of Efficiency, Stability and Recovery Future Perspectives, Chapter 5, Water Purification, Nova science Publ., NY (2009) 4th Quarter. ISBN: 978-1-60741-599-2.
36. H. S. Hilal, G. Y. M. Nour and A. Zyoud, Photo-Degradation of Methyl Orange with Direct Solar Light using ZnO and Activated Carbon-Supported ZnO, Chapter 6, Water Purification, Nova science Publ., NY (2009) 4th Quarter. ISBN: 978-1-60741-599-2.
37. J. P. Percherancier, R. Chapelion and B. Pouyet, "**Semiconductor Sensitized Photodegradation of Pesticides in Water: The Case of Carbetamide**". *J. Photochem. Photobiol. A: Chem.*, **87** (1995); 261-265.
38. I. Poullos, M. Kositzi, A. Kouras, "**Photocatalytic Decomposition of Trichlopyr over Aqueous Semiconductor Suspensions**". *J. Photochem. Photobiol. A: Chem.*; **115** (1998) 175.
39. M. C. Yeber, J. Rodriguez, J. Freer, J. Baeza, N. Duran and H. D. Mansilla, "**Advanced Oxidation of a Pulp Mill Bleaching Wastewater**". *Chemosphere*, **39** (1999); 1679-1683.

40. A. A. Khodja, T. Sehili, J. F. Pilichowski and P. Boule, "**Photocatalytic Degradation of 2-phenylphenol on TiO₂ and ZnO in Aqueous Suspensions**". *J. Photochem. Photobiol A: Chem*, **141** (2001); 231-236.
41. C. Marci, V. Augugliaro, M. J. L. Munoz, C. Martin, L. Palmisano, V. Rives, M. Sehhiavello, R. J. D. Tilley and A. M. Venezia, "**Preparation Characterization and Photocatalytic Activity of Polycrystalline ZnO/TiO₂ Systems**". *J. Phys. Chem. B*, **105** (5) (2001); 1026-1032.
42. C. Lizama, J. Freer, J. Baeza, H.D. Mansilla, "**Optimized photodegradation of Reactive Blue 19 on TiO₂ and ZnO suspensions**". *Catal. Today* **76** (2002); 235.
43. N. Daneshvar, D. Salari and A. R. Khataee, "**Photocatalytic Degradation of Azo Dye Acid Red 14 in Water on ZnO as an Alternative Catalyst to TiO₂**". *J. Photochem. Photobiol A: Chem*, **162** (2004); 317-322.
44. K. Gouvea, F. Wypych, S. G. Moraes, N. Duran, N. Nagata and P. Peralta-Zamora, "**Semiconductor-Assisted Photocatalytic Degradation of Reactive Dyes in Aqueous Solution**". *Chemosphere*, **40** (2000); 433-440.
45. R. Y. Hong, T. T. Pan, J. Z. Qian and H. Z. Li, "**Synthesis and Surface Modification of ZnO Nanoparticles**". *Chem. Eng. J.* **119** (2006) 71-81.
46. R. Y. Hong, J. Z. Qian and J. X. Cao, "**Synthesis and Characterization of PMMA Grafted ZnO Nanoparticles**". *Powder Technol*, **163** (2006); 160-168.
47. R. Y. Hong, L. L. Chen, J. H. Li, H. Z. Li, Y. Zheng and J. Ding, "**Preparation and Application of Polystyrene-Grafted ZnO Nanoparticles**". *Polym. Adv. Technol.*, **18** (11) (2007); 901-909.
48. S. Talam, S. R. Karumuri, N. Gunnam, "**Synthesis, Characterization, and Spectroscopic Properties of ZnO Nanoparticles**". *ISNR Nanotech.*, **2012** (2012); 6.
49. http://www.unitconversion.org/unit_converter/illumination.html.

50. <http://www.svetila.com/en/ultra-vitalux-300w-1170.html>,
(accessed 28 July 2011).

51. J.A MacLaughlin, R.R. Anderson and M.F.Holick, "**Spectral character of sunlight modulates photosynthesis of previtamin D3 and its photoisomers in human skin**". *Science*. **216** (1982) 1001-1003.

52. A. Drici, G. Djeteli, G. Tchangbedji, H. Derouiche, , K. Jondo, K. Napo, J. C. Berne` de, S. Ouro-Djobo and M. Gbagba, "**Structured ZnO thin films by chemical bath deposition for photovoltaic applications**". *phys. Status Solidi a*, **201** (7) (2004) 1528–1536.

53. J. Ouerfelli, M. Regragui, M. Morsli, G. Djeteli, K. Jondo, C. Amory, G. Tchangbedji, K. Napo4 and J. C. Bern`ede, "**Properties of ZnO thin films deposited by chemical bath deposition and post annealed**". *J. Phys. D: Appl. Phys.* **39** (2006); 1954–1959.

54. M. N. Daneshvar, S. Aber, M. S. Seyed Dorraji, A. R. Khataee, and M. H. Rasoulifard, "**Preparation and Investigation of Photocatalytic Properties of ZnO Nanocrystals: Effect of Operational Parameters and Kinetic Study**". *Int. J. Chem. Biomol. Eng.* **1** (2008); 24-29.

55. http://www.nanomt.com/sc_zno.asp. Accessed 24 SEP 2011.

56. I. Poullos, A. Avranas, E. Rekliti, A Zouboulis, "**Photocatalytic oxidation of Auramine O in the presence of semiconducting oxides**". *J. Chem. Technol. Biotechnol.* **75** (2000); 205.

57. I. Poullos, M. Kositzi, A. Kouras, "**Photocatalytic decomposition of triclopyr over aqueous semiconductor suspensions**". *J. Photochem. Photobiol. A: Chem.* **115** (1998); 175.

58. A. B Prevot, M.Vincenti, A. Bianciotto, E. Pramauro, "**Photocatalytic and photolytic transformation of chloramben in aqueous solutions**". *Appl. Catal. B: Environ.* **22** (1999); 149.

59. S. Sakthivel, B. Neppolian, M. V. Shankar, B. Arabindoo, M. Palanichamy, V. Murugesan, "**Solar photocatalytic degradation of azo dye comparison of photocatalytic efficiency of ZnO and TiO₂**". *Sol. Energy Mater. Sol. Cells* **77** (2003); 65.

60. C. Lizama, J. Freer, J. Baeza, H. D. Mansilla, "**Optimized Photodegradation of Reactive Blue 19 on TiO₂ and ZnO suspensions**". *Catal. Today* **76** (2002); 235–246.

61. A. Piscopo, D. Robert, J. V. Weber, **"Influence of pH and chloride anion on the photocatalytic degradation of organic compounds Part I. Effect on the benzamide and para-hydroxybenzoic acid in TiO₂ aqueous solution"**. *Appl.Catal. B: Environ.* **35** (2001); 117.
62. D. S. Bhatkhande, V. G. Pangarkar, A. Beenackers, **"Photocatalytic degradation for environmental applications-a review"**. *J. Chem. Technol. Biotechnol.* **77** (2001); 102.
63. M-C. Lu, G. D. Roam, J. N. Chen, C. P. Huang, **"Factors affecting the photocatalytic degradation of dichlorovos over titanium dioxide supported on glass"**. *J. Photochem. Photobiol. A: Chem.* **76** (1993); 103.
64. L. Jianguo, G. Wanbing, H. Kai, Z. Jianbo, M. Fanming, S. Xueping, S. Zhaoqi, **"Effect of annealing temperature on photocatalytic activity of ZnO thin films prepared by sol-gel method"**. *Superlattices Microstruct.* **50** (2011); 98–106.
65. W. Huihu, X. Changsheng, **"Effect of annealing temperature on microstructures and photocatalytic property of colloidal the ZnO nanoparticles"**. *J. Phys. Chem. Solids* **69** (2008); 2440-2444.
66. M. Okorn, P. Pongsapak, P. Piyasan, P. Joongjai, **"Effects of synthesis conditions and annealing post-treatment on the photocatalytic activities of ZnO nanoparticles in the degradation of methylene blue dye"**. *Chem. Eng. J* **164** (2010); 77-84.
67. F. PENG, S. CHEN, L. ZHANG, H. WANG, Z. XIE, **"Preparation of Visible-light Response Nano-sized ZnO Film and its Photocatalytic Degradation to Methyl Orange"**. *Acta Phys. -Chim. Sin.*, **21(9)** (2005), 944-948.
68. P. Spathis, I. Poullos, **"The corrosion and photocorrosion of zinc and zinc oxide coatings"**. *Corros. Sci.* **37** (1995); 673-680.
69. Y. Bessekhoud, N. Chaoui, M. Trzpit, N. Ghazzal, D. Robert, J. V. Weber, **"UV-vis versus visible degradation of Acid Orange II in a coupled CdS/TiO₂ semiconductors suspension"**. *J. Photochem. Photobiol. A*, **183** (2006); 218–224.
70. O. Carp, C. Huisman, and A. Reller, **"Photo-induced reactivity of TiO₂"**. *Progr. Solid state Chem.* **32** (2004); 33-177.

71. J. M. Hermann, "**Heterogeneous photocatalysis: fundamentals and applications to the removal of various types of aqueous pollutants**". *Catal. Today*, **53** (1999); 115-129.
72. N. Guettai, H. A. Amar, "**Photocatalytic oxidation of methyl orange in presence of titanium dioxide in aqueous suspension. Part I: Parametric study**". *Desalination*, **185** (2005); 427-437.
73. Y. Bessekhoud, D. Robert, J. V. Weber, "**Bi₂S₃/TiO₂ and CdS/TiO₂ heterojunctions as an available configuration for photocatalytic degradation of organic pollutant**". *J. Photochem. Photobiol. A*, **163** (2004); 569–580.
74. O. Carp, C. L Huisman, A. Roller, "**Photoinduced reactivity of titanium dioxide**". *Prog. Solid State Che.*, **32** (2004); 33.
75. A. H. Zyoud, N. Zaatar, I. Saadeddin, C. Ali, D. Park, G. Campet, H. S. Hilal, CdS-sensitized TiO₂ in phenazopyridine photo-degradation: Catalyst efficiency, stability and feasibility assessment, *J. Hazard. Mater.*, **173** (2010); 318–325.
76. A. Zyoud, N. Zaatar, I. Saadeddin, M. H. Helal, G. Campet, M. Hakim, D-H. Park, H. S. Hilal, Alternative natural dyes in water purification: Anthocyanin as TiO₂-sensitizer in methyl orange photo-degradation, *Solid State Sci.*, **13** (2011); 1268-1275.
77. Ahed Zyoud, Nidal Zatar, Hikmat Hilal Nanoparticle CdS-Sensitized TiO₂ Catalyst for Photo-Degradation of Water Organic Contaminants: Feasibility Assessment and Natural-Dye Alternatives, Ph. D. Thesis, An-Najah National University, Palestine, 2009, 155.
78. Ahed H Zyoud, Nidal Zater, Iyad Saadeddin, Moath Helal, Ghazi Noor, Hikmat S Hilal, Photodegradation of Water Organic Contaminates Under Solar Simulator Light, **The Fifth Palestinian International Chemistry Conference**, An-Najah National University, Palestine, 2009.
79. M. Qamar, M. Muneer, D. Bahnemann, "**Heterogeneous photocatalysed degradation of two selected pesticide derivatives, triclopyr and daminozid in aqueous suspensions of titanium dioxide**". *J. Environ. Management*, **80** (2006); 99–106.

80. C. Karunakaran, S. Senthilvelan, "**Photooxidation of aniline on alumina with sunlight and artificial UV light**". *Catal. Commun.* **6** (2005); 159–165.
81. C. Minero, D. Vione, "**A quantitative evaluation of the photocatalytic performance of TiO₂ slurries**". *Appl. Catal. B* **67** (2006) 257-269.
82. N. Serpone, G. Sauvé, R. Koch, H. Tahiri, P. Pichat, P. Piccinini, E. Pelizzetti, H. Hidaka, "**Standardization protocol of process efficiencies and activation parameters in heterogeneous photocatalysis: relative photonic efficiencies ζ_r** ". *J. Photochem. Photobiol. A* **94** (1996); 191–203.
83. M. A. Aguado, M. A. Anderson, C. G. Hill Jr., "**Influence of light intensity and membrane properties on the photocatalytic degradation of formic acid over TiO₂ ceramic membranes**". *J. Mol. Catal.* **89** (1994); 165–178.
84. C. G. Silva, W. Wang, J. L. Faria, "**Photocatalytic and photochemical degradation of mono-, di- and tri-azo dyes in aqueous solution under UV irradiation**". *Photochem. Photobiol. A* **181** (2006); 314–324.

جامعة النجاح الوطنية

كلية الدراسات العليا

حفازات حبيبات أكسيد الزنك النانوية في تحطيم الملوثات بالضوء الشمسي

أهمية تثبيت الحفاز

إعداد

حسام أحمد عبد الله عامر

إشراف

أ.د. حكمت هلال

قدمت هذه الأطروحة استكمالاً لمتطلبات الماجستير في الكيمياء بكلية الدراسات العليا في جامعة النجاح الوطنية، نابلس- فلسطين .

2012

ب

حفازات حبيبات أكسيد الزنك النانوية في تحطيم الملوثات بالضوء الشمسي: أهمية تثبيت الحفاز

إعداد

حسام أحمد عبدالله عامر

إشراف

أ.د. حكمت هلال

الملخص

إن أكسيد الزنك من أشباه الموصلات التي تمتلك فجوة طاقة (Energy Band) واسعة نسبياً ، وحتى تنتقل الإلكترونات من حزمة التكافؤ (Valence Band) إلى حزمة التوصيل (Conducting Band) فإنها بحاجة إلى ضوء بامواج قصيرة نسبياً فوق البنفسجية. هذا ومن المناسب استخدام الطاقة الشمسية في التحطيم الضوئي لملوثات مختلفة لعدة أسباب، آخذين بالاعتبار أن جزءاً يسيراً من الإشعاع الشمسي الذي يصلنا يمتلك امواجاً ضمن الأشعة فوق البنفسجية. إن القدرة العالية لأكسيد الزنك على امتصاص الأشعة فوق البنفسجية تجعله فعالاً للاستخدام في التحطيم الضوئي، علاوة على كونه رخيص الثمن ومتوفرأً ولا يشكل خطورة .

لقد تم استخدام أكسيد الزنك المنفرد والمثبت على سطوح الرمل والفخار والكربون كحفاز ضوئي في تحطيم ملوث من صبغة الميثيل البرتقالي، بضوء الشمس المباشر و باستخدام لمبات الأشعة فوق البنفسجية. وقد تم استخدام مطيافية الضوء المرئي وفوق البنفسجي و قياسات مطيافية الوميض وتمثيل الأشعة السينية وصورالميكروسكوب الإلكتروني الماسح في تحليل أكسيد الزنك المنفرد والمثبت على الأسطح، ثم تمت دراسة سرعة تفاعل التحطيم الضوئي تحت ظروف مختلفة من حيث درجة الحموضة ودرجة الحرارة وتركيز الحفاز وتركيز الملوث علاوة على تركيز شدة الإضاءة، وطبيعة الحفاز ونوع المثبت. تبين أن سرعة التفاعل كانت أفضل في المحلول المتعادل منها في الوسط الحمضي أو القاعدي، كذلك فإن زيادة كمية الحفاز عملت على زيادة سرعة تفاعل التحطيم حتى كميات محددة وعند إضافة كميات إضافية لم يلاحظ زيادة اخرى في السرعة. أما زيادة تركيز الملوث فقد أدت إلى زيادة معدل سرعة التفاعل. وبالنسبة لزيادة درجة حرارة وسط التفاعل فقد أظهرت تأثيراً قليلاً في سرعة التفاعل وذلك بسبب صغر طاقة التنشيط التي تم حسابها. هذا وقد تم تسريع عملية التحطيم عن طريق تركيز الضوء الشمسي باستخدام المرايا المقعرة.

علاوة على ذلك فقد تم دراسة أنواع مختلفة من ZnO التجارية والمحضرة حيث عملت جميعا على تحطيم كامل للملوث بعد فترة زمنية كافية. أما أكسيد الزنك المثبت على الكربون المنشط فقد أظهر أفضل فعالية من بين الحفازات المستخدمة في تحطيم الملوث. وتبيّن كذلك أنه يمكن تحسين فعالية الحفاز بواسطة شوائبه قبل استخدامه. بناء على ذلك فقد تم التوصل الى خلاصة مفادها ان اكسيد الزنك يصلح للاستخدام كحفاز في تحطيم الملوثات العضوية في الماء بواسطة الاشعة الشمسية المباشرة.